

The possibility of superparamagnetic iron oxide nanoparticles as positive contrast agents in low-field MRA

K. Wieriks

MSc Thesis BME
December 2022

Supervisors:
Prof. dr. ir. B. ten Haken
Dr. ir. F.F.J. Simonis
Dr. E. Groot Jebbink



PREFACE

This thesis is the final assignment to complete the master of Biomedical Engineering, specifically the Imaging and In Vitro Diagnostics track. This research is conducted at the Magnetic Detection and Imaging (MD&I) group. The graduation committee includes prof. dr. ir. B. ten Haken (chair), F.F.J. Simonis (daily supervisor) and dr. E. Groot Jebbink (external member).

Firstly, I want to thank my daily supervisor F.F.J. Simonis (Frank), for his involvement and guidance during this project. His ongoing enthusiasm and expertise in MRI inspired me and made me feel excited and motivated to work on the research project. Secondly, I want to thank all other students from our 'Master room', especially Saskia Damen and Marleen Krommendijk, for the nice coffee breaks and the offered help if needed. Lastly, I want to thank my friends, family and girlfriend, who supported me over the last year.

ABSTRACT

Purpose: Low-field magnetic resonance imaging (MRI) gives rise to opportunities in interventional MRI, like magnetic resonance angiography (MRA). Good contrast agents are essential in MRA. However, the now-used gadolinium-based contrast agents are not efficient at low-field. Superparamagnetic iron oxide nanoparticles (SPIONs) could provide a good alternative. However, their use as positive contrast agent needs to be examined. Therefore, this study investigates the possibility of using SPIONs as positive contrast agents in low-field MRA.

Methods: This study investigates the relaxivity of three SPIONs at field strengths of 0.25, 0.5 and 1.5T. First, it is investigated how relaxivity is determined robustly and how it can be measured at the available scanners. Protocols were designed for each field's strength, and the temperature dependency of relaxivity was investigated. Relaxivity is measured at clinically relevant conditions, e.g., at 37°C and in a blood medium. With these relaxivities, relaxivity ratios are calculated. These give a measure of the type of contrast, which can be positive or negative.

Results: Contrast agent relaxivity was found to be temperature dependent, whereas a lower temperature would induce a higher relaxivity. This research found that the longitudinal relaxivities at a field strength of 1.5T are at least two times lower than a field of 0.25T and even five times lower than 0.5T. The transverse relaxivities at a field strength of 1.5T are lower than 0.25 and 0.5T. The relaxivity ratio of SPIONs is meagre at 1.5T, which results in negative contrast. At lower fields, this ratio is higher, with the highest ratio at a field strength of 0.25T.

Conclusion: It is essential to measure the relaxivity of contrast agents at a clinically relevant temperature of 37°C. If a lower temperature were used, the measured relaxivity would be overestimated. Furthermore, this research concludes that SPIONs can be used as positive contrast agents due to their relaxivity ratio at low magnetic field strengths. This ratio is SPION-dependent. Because of the positive contrast and prolonged circulation time SPIONs could be a viable alternative to gadolinium-based contrast agents in low-field MRA.

SAMENVATTING

Doel: Laagveld magnetic resonance imaging (MRI) brengt mogelijkheden op het gebied van interventionele MRI, zoals bijvoorbeeld magnetic resonance angiography (MRA). Goede contrastmiddelen zijn essentieel in MRA. Echter zijn de huidige, op gadolinium gebaseerde, contrastmiddelen niet efficiënt op laagveld. Superparamagnetic iron oxide nanoparticles (SPIONs) kunnen een mogelijk alternatief bieden. Echter moet het gebruik van SPIONs als positief contrastmiddel nog onderzocht worden. Daarom wordt in dit onderzoek de mogelijkheid van het gebruik van SPIONs als positief contrastmiddel bij laagveld MRA onderzocht.

Methode: Dit onderzoek onderzoekt de relaxiviteit van drie verschillende SPIONs op veldsterktes van 0.25, 0.5 en 1.5T. Eerst zal worden onderzocht hoe de relaxiviteit robuust kan worden bepaald op elke scanner. Protocollen zijn ontworpen voor elke veldsterkte en de afhankelijk van temperatuur van de relaxiviteit is onderzocht. Vervolgens is de relaxiviteit gemeten onder klinisch relevant omstandigheden, dat wil zeggen in bloed en op 37°C. Met deze relaxiviteiten, kunnen de relaxiviteits ratio's van de SPIONs bepaald worden. Deze verhoudingen geven een mate van het type contrast, welke positief of negatief kan zijn.

Resultaten: Als resultaat is gevonden dat de relaxiviteit van contrastmiddelen afhankelijk is van de temperatuur. Een lagere temperatuur resulteert in een hogere relaxiviteit. Tevens is een resultaat van dit onderzoek dat de longitudinale relaxiviteit op een veldsterkte van 1.5T minstens twee keer lager zijn dan bij een veldsterkte van 0.25T en zelf 5 keer lager bij een veldsterkte van 0.5T. De transversale relaxiviteit op een veldsterkte van 1.5T zijn tevens lager dan bij veldsterktes van 0.25 en 0.5T. Het relaxiviteits ratio van SPIONs is matig op 1.5T, wat resulteert in negatief contrast. Echter op lage veldsterktes is dit ratio hoger, met het hoogste ratio gemeten op een veldsterkte van 0.25T.

Conclusie: Het is essentieel om de relaxiviteit te meten van contrastmiddelen op een klinisch relevante temperatuur van 37°C. Op een lagere temperatuur zal de meting van de relaxiviteit worden overschat. Ook kan met dit onderzoek worden geconcludeerd dat SPIONs een optie zijn als positieve contrastmiddelen vanwege hun gunstige relaxiviteits ratio op laagveld. Dit ratio is echter wel SPION afhankelijk. Vanwege het positieve contrast en vanwege de lange circulatietijd zijn SPIONs een waardig alternatief voor gadolinium gebaseerde contrastmiddelen in laagveld MRA.

Contents

Preface.....	2
Abstract	3
Samenvatting.....	4
Abbreviations	7
1 Introduction.....	8
1.1 Research question	9
1.2 Structure of the report	9
2 Theoretical background.....	10
2.1 Basic principles MRI.....	10
2.2 Contrast agents	11
2.2.1 Relaxivity	11
2.2.2 Relaxivity mechanisms	11
2.3 Measuring relaxivity	13
2.3.1 T ₁ determination	13
2.3.2 T ₂ determination	13
2.3.3 Calculation of the relaxivity	14
3 Relaxivity protocol development for each field strength.....	16
3.1 Measurements at 0.5T	16
3.1.1 Initial measurement steps.....	16
3.1.2 Optimisation steps.....	17
3.2 Measurements at 1.5T	17
3.2.1 Initial measurement steps.....	18
3.2.2 Optimisation steps.....	18
3.3 Measurements at 0.25T	19
3.3.1 Initial measurement steps.....	19
3.3.2 Optimisation steps.....	20
3.4 Discussion	20
4 Effect of temperature on relaxivity	21
4.1 Introduction.....	21
4.2 Materials.....	21
4.3 Method	21
4.4 Results	22
4.5 Discussion	23
4.6 Conclusion	23

5	SPION relaxivity measurements at each field strength.....	24
5.1	Materials.....	24
5.1.1	SPION selection for relaxivity measurements	24
5.1.2	Dilution medium.....	24
5.1.3	SPION sample fabrication.....	24
5.2	Method.....	25
5.2.1	Protocol specifications	25
5.2.2	Scanning parameters.....	25
5.2.3	Temperature regulation	26
5.2.4	Scanning procedure.....	26
5.3	Results	27
5.3.1	EMG304	27
5.3.2	SPH25.....	28
5.3.3	SynomagD50.....	29
5.3.4	Relaxivity ratios	30
5.4	Discussion	30
5.4.1	EMG304	30
5.4.2	SPH25.....	31
5.4.3	SynomagD50.....	31
5.4.4	Relaxivity ratios	32
5.5	Conclusion	33
6	General discussion.....	34
6.1	Background.....	34
6.2	Temperature measurement.....	34
6.3	Protocol development.....	34
6.4	SPION & sample selection	35
6.5	Results section.....	35
6.6	Overall	35
6.7	Future work & recommendations	36
7	Conclusion	38
	References.....	39
8	Appendices	43
8.1	Appendix A: Scanner protocols	43
8.2	Appendix B: SPION preliminary tests	47
8.2.1	Results and discussion preliminary relaxivity measurements.....	47

ABBREVIATIONS

CPMG	Carr-Purcell-Meiboom-Gill
ETL	Echo train length
FOV	Field of view
FSE	Fast spin echo
IR	Inversion recovery
MRA	Magnetic resonance angiography
MRI	Magnetic resonance imaging
Multi-SE	Multi spin echo
r_1	Longitudinal relaxivity
r_2	Transversal relaxivity
RF-pulse	Radiofrequency pulse
ROI	Region of interest
SNR	Signal-to-noise ratio
SPIO	Superparamagnetic iron oxide nanoparticle
T_1	Longitudinal relaxation time
T_{1e}	Estimated T_1
T_2	Transversal relaxation time
TE	Echo time
TI	Inversion time
TR	Repetition time

1 INTRODUCTION

Since the introduction of magnetic resonance imaging (MRI) in the hospital, field strengths have increased. Where the first scanners started with a field strength of 0.05 to 0.35 Tesla (T), most common scanners have risen to a field strength of 1.5 or 3T [1]. Even higher fields of 7 and 11T are still being researched or used in hospitals [2]. These high field strengths (field strengths of 1.5T and above) induce higher polarisation, which is used to get higher image quality or a higher spatial resolution because of an increase in signal-to-noise ratio (SNR). Nevertheless, these high fields also have a downside, including higher costs, specific absorption rate limitations, and increasing operating complexity. Because of the high costs of high-field scanners, they are not accessible to every hospital, especially in underdeveloped countries [3]. Furthermore, the increasing image quality of these high fields is not always needed; diagnoses can also be made on low-field acquisitions [4].

Low-field scanners (field strength below 1.5T) could be an alternative because the weaker magnet is cheaper concerning manufacturing and maintenance. The interest in low-field MRI is rising because of the flexibility that comes with the weaker magnets. Weaker magnets can produce scanners with limited constraints regarding scanner design, which will give the possibility for research applications like upright imaging. Furthermore, low-field MRI brings opportunities in interventional MRI, like MRI guidance or cardiovascular procedures [5]. One of these cardiovascular procedures in imaging the blood vessels is called magnetic resonance angiography (MRA) [6].

In MRA, a contrast agent is injected intravenously, and after some delay, the blood vessels can be scanned and reconstructed in an image called an angiogram. The most common contrast agents used at high-field MRA are based on the element gadolinium because of its paramagnetic properties [7]. The effect of a contrast agent is dependent on the field strength. The effect of gadolinium in low-field is less than in high-field; therefore, a higher dose is needed to create the same contrast enhancement [1]. This decrease in contrast difference is due to the shorter relaxation times at low fields, resulting in a drop in the contrast-to-noise ratio [8]. However, a higher dose of a gadolinium contrast agent would not be preferable because of its association with nephrogenic systemic fibrosis (NSF) for patients with renal dysfunction [9]. The time in which a gadolinium contrast agent circulates in the body before it is secreted is also limited; therefore, it is essential to image the enhanced blood vessels at the right moment.

Other contrast agents than gadolinium might be used at low-field MRI, for example, superparamagnetic iron oxide nanoparticles (SPIONs). SPIONs have a high magnetic moment, and prolonged circulation time in blood vessels, which increases the time the blood vessels can be imaged. This increased circulation time is due to their small size [10]. Furthermore, SPIONs can be coated to target specific areas in the human body. Contrast agents can induce positive contrast and increase the MRI signal or induce negative contrast and lower the signal. For most MRI applications and likewise for MRA, positive contrast is preferred. To induce positive contrast, the characteristics of the contrast agent should be suitable. SPIONs are already used at high fields as negative contrast agents, which results in lower signal, but it is hypothesised that they could be used as positive contrast agents at lower magnetic fields [8]. This positive contrast behaviour of SPIONs depends on multiple factors, whereas the size of the SPION is proposed to have the most decisive influence.

1.1 RESEARCH QUESTION

It is now well established that SPIONs can be used as contrast agents in MRI. However, the behaviour of SPIONs as positive contrast agents in low-field MRI is still not fully understood. This indicates a need to investigate the contrast behaviour of SPIONs in low-field. Prolonged circulation times make SPIONs a good option for MRA. However, to use SPIONs in MRA, they need to induce positive contrast. Therefore, this research aims to assess the contrast-enhancing capability of SPIONs at low-field MRA.

The main question in this research is whether SPIONs can be used as a positive contrast agent in low-field MRA.

To answer the question, the contrast behaviour of SPIONs will be investigated at three different field strengths, 0.25, 0.5 and 1.5T. To get an insight into essential features of SPION contrast enhancement, three different SPIONs will be used, differentiated by core diameter. Various influential parameters will be investigated to ensure robust and accurate measurements. To ensure clinical relevancy, porcine blood will be used as a medium. Furthermore, measurements will be performed at 37°C to mimic the human body temperature.

1.2 STRUCTURE OF THE REPORT

This report has been organised in the following way: The next chapter briefly reviews the basic principles of MRI and a theoretical background about MRI contrast agents. The section ends with explaining the different steps for relaxivity determination. Chapter 3 describes the experimental approach and instrumentation utilised in developing protocols for the relaxivity measurement at each field strength. The main focus of this chapter is the adjustments made in the 0.25T protocol. The fourth chapter describes the effect of temperature on longitudinal relaxivity measurements. Chapter 5 presents the results of the relaxivity measurements of three SPIONs. The first section of this chapter discusses the materials and methods for executing the relaxivity measurements, whereafter the results for each SPION are discussed separately. Lastly, the relaxivity ratios of each SPION are calculated and discussed. The final chapters 6 and 7 contain the discussion and the conclusion. Chapter 6 draws together the key findings, first making a statement for each previous chapter, where a general discussion of the research follows. Chapter 7 summarises this research's main findings and identifies further research areas.

2 THEORETICAL BACKGROUND

This chapter contains the technical background of this research. First, the paper explains the basic principles of MRI. After that, the use of different contrast agents is outlined. Lastly, the technical background of the used MRI sequences is given.

2.1 BASIC PRINCIPLES MRI

Magnetic resonance imaging (MRI) works on the principle of imaging the magnetisation of hydrogen atoms. These atoms have a spin, and when these atoms are introduced inside a magnetic field, the spins of the water atoms will align with the magnetic field. More of these spins are oriented along the field, which results in a net magnetisation along the axis of the magnetic field (B_0). By introducing another pulsed magnetic field (B_1) in the form of a radiofrequency pulse (RF-pulse), the spins are rotated away from their parallel orientation and will precess. This RF-pulse needs to be applied at the right frequency to get this result, called the Larmor frequency. After this RF-pulse, the spins relax back to the equilibrium state. The rate at which this happens is tissue-dependent and is called relaxation. There are two types of relaxation, longitudinal (along the M_z axis) and transversal relaxation (along the M_{xy} axis). Longitudinal relaxation (T_1), also called thermal relaxation or spin-lattice relaxation, states how the net magnetisation returns to equilibrium. Transverse relaxation (T_2), also called spin-spin relaxation, is how the transverse components of the magnetisation decay after the RF-pulse. The decay of this signal happens due to the dephasing of the spins. This dephasing is caused by local interactions between the spins and macroscopic effects, like field inhomogeneities. When the spins are in the transverse plane, their components and vector sum will precess within this plane. This sweep of magnetisation induces the current that the receiver coils will measure and is therefore responsible for generating the MR signal. Relaxation can be modelled using Bloch equations, which results in the equations stated below [11]. In these equations, ω_0 stands for the Larmor frequency, and α stands for the flip angle of the RF-pulse.

$$M_z(t) = M_0 \left(1 - e^{-\frac{t}{T_1}} \right) + M_0 \cdot \cos(\alpha) \cdot e^{-\frac{t}{T_1}} \quad (1)$$

$$M_{xy}(t) = M_0 \cdot \sin(\alpha) \cdot e^{-j\omega_0 t} \cdot e^{-\frac{t}{T_2}} \quad (2)$$

The T_1 and T_2 of a particular tissue determine the contrast in an MRI image. Small molecules, like water, have a wide range of molecular tumbling rates [12]. This wide range matches the Larmor frequency poorly, resulting in long T_1 . Medium-size molecules, like lipids, have a narrower range of tumbling rate, which better matches the Larmor frequency and results in short T_1 . However, large molecules, like protein and DNA, have a very slow tumbling rate and do not reach the Larmor frequency, resulting in long T_1 . T_2 is related to the tumbling rate. Large molecules with a slow tumbling rate have short T_2 .

Because the relaxation times depend on the Larmor frequency, they also depend on the used field strength. In literature, it is found that with increasing field strength, T_1 increases and T_2 decreases [3]. Therefore, on lower fields, the T_1 and T_2 are closer together than at high fields, making it harder to obtain the required contrast level.

2.2 CONTRAST AGENTS

Contrast agents are used for enhancing contrast in MRI. In MRA, contrast agents increase the signal acquired from blood vessels. They could also increase the signal strength of specific tissue types, like tumours [13]. These contrast agents must have specific chemical properties and a suitable pharmacokinetic profile so they are not toxic to the human body [14].

2.2.1 Relaxivity

As mentioned in the introduction, contrast agents can induce positive contrast by increasing the signal intensity or induce negative contrast by decreasing the signal intensity. Inducing contrast is done indirectly; the contrast agent does not become visible by itself but modifies the relaxation times of its surroundings [15]. When a contrast agent has a large magnetic moment, it alters the surrounding tissues' magnetic field, creating a large magnetic field heterogeneity through which water molecules diffuse. Diffusion causes dephasing, which results in the shortening of T_2 . The rate at which a contrast agent influences the relaxation time is called relaxivity [16]. Relaxivity gives the efficiency of the contrast agent and is given in $mM^{-1}s^{-1}$. Relaxivity is defined as the linear regression slope generated from a plot of the inverse relaxation time versus the concentration of the contrast agent [17]. A lower dose of a high relaxivity contrast agent is needed for the same contrast compared to a low relaxivity contrast agent [18]. Because a contrast agent can individually affect the T_1 and T_2 , there are two relaxivities, r_1 for T_1 and r_2 for T_2 . The relation between T_1 and T_2 and their corresponding relaxivities is given in the following equation:

$$R_i(C) = \frac{1}{T_i(C)} = \frac{1}{T_i(0)} + r_i \cdot [C]; \quad i = 1,2 \quad (3)$$

Where $R_i(C)$ is the global relaxation rate with the contrast agent (s^{-1}), $T_i(C)$ is the relaxation time with the contrast agent (s), $T_i(0)$ is the initial relaxation time without the contrast agent (s), r_i is the relaxivity ($mM^{-1}s^{-1}$), and C is the concentration of the contrast agent (mM). Next to this relaxivity value, other factors also influence the efficiency of the contrast agent and the signal enhancement, such as contrast agent distribution, proton density, diffusion and chemical environment. Therefore, contrast enhancement depends not only on the used contrast agent but also on the enhanced tissue or fluid. The type of contrast (negative or positive) depends on the ratio between the longitudinal and transverse relaxivity (r_1/r_2). The higher the ratio, the better suited the contrast agent for T_1 enhancement in MRA [19].

2.2.2 Relaxivity mechanisms

The relaxivity of a contrast agent depends on the core's magnetisation type. This magnetisation can be paramagnetic or superparamagnetic. Paramagnetic and superparamagnetic materials can become temporarily magnetised when placed in an external magnetic field.

2.2.2.1 Paramagnetic relaxation

The most commonly used contrast agents are based on gadolinium, which is paramagnetic due to its seven unpaired electrons. The dipole-dipole interactions between water protons and the paramagnetic centre cause paramagnetic relaxation. The biophysical factors influencing how strong paramagnetic contrast agents affect the relaxivity can be simplified into inner-sphere and outer-sphere mechanisms. Inner-sphere mechanisms relate to the interactions between water molecules and the paramagnetic centre at a distance below 0.3 nm. The number of interactions depends on the size and shape of the paramagnetic contrast agents. The outer-sphere mechanism relates to the interactions between the water molecules at a distance of 0.4 to 0.5 nm from the paramagnetic centre. These interactions are not as powerful as the inner-sphere effects.

The inner- and outer-sphere mechanisms depend on the applied field strength, the size of the contrast agents, the temperature, the type of the contrast agent and the diffusion rate of the surrounding water. For gadolinium-based contrast agents, inner- and outer-sphere contributions are the same at field strengths between 0.5 and 3.0 T. However, outer-sphere interactions become more critical at lower field strengths and for smaller contrast agents. Emphasising the interest in using SPIONs at low-field.

2.2.2.2 *Superparamagnetic relaxation*

Superparamagnetic relaxation is affected by the same mechanisms as paramagnetic relaxation. However, another second sphere contribution is added due to the interactions between water molecules and the surface coating. Superparamagnetic particles show saturation magnetisation values much higher than paramagnetic particles at equal magnetic field strength, increasing transversal relaxivity effects. [20].

As the name already suggests, SPIONs have a superparamagnetic core. SPIONs are particles of nano size which are formed of tiny crystals of iron oxide. Magnetite (Fe_3O_4) and maghemite ($\gamma\text{-Fe}_2\text{O}_3$) are the most common of these iron oxides [21]. To make the crystals stable in aqueous media, the surface of the crystals can be modified. This modification can be done by capping the SPIONs with different coatings such as organic acids, hydrophilic polymers and polysaccharides. A SPION has a core-shell structure, where the surface spins are disordered in the outer layer. The spins in the core of the SPIONs contribute to the magnetisation; therefore, a bigger core size results in larger magnetisation, which increases the transversal relaxivity effects [22]. Therefore, smaller SPIONs are more favourable for T_1 contrast because of the higher r_1/r_2 ratio. However, a tiny core size also means a high chance of aggregation, which is not preferable [23].

Nevertheless, a benefit of the small size of SPIONs is their elimination from blood circulation. Instead of remaining in the extracellular space like gadolinium, SPIONs are taken up by the reticuloendothelial system cells in the liver, spleen, bone marrow, and lymph nodes and are phagocytosed by the macrophages throughout the body. Due to this, SPIONs remain in the blood between 1 to 24-36 hours before being cleared out [24].

2.3 MEASURING RELAXIVITY

The relaxivity ratio (r_1/r_2) must be known to investigate whether a contrast agent can induce positive contrast. A high ratio is more favourable for achieving positive contrast. Therefore, the longitudinal and transverse relaxivity must be determined. Relaxivity is defined as the linear regression slope generated from a plot of the inverse relaxation time versus the concentration of the contrast agent [17]. Several methods can measure T_1 and T_2 .

2.3.1 T_1 determination

The most common method to measure T_1 is by using inversion recovery [25]. An inversion recovery (IR) sequence consists of two pulses: it starts with a 180° pulse followed by a 90° pulse after a specific delay time. This delay time is called the inversion time (TI). When measuring the MR signal at different TI, the T_1 can be fitted to that data with the following equation:

$$S = M_0 \left(1 - 2e^{-\frac{TI}{T_1}} \right) + a \quad (4)$$

Other methods to estimate the T_1 are also used, namely Look-Locker and Variable flip angle (VFA). However, IR is the golden standard for doing T_1 estimation [26].

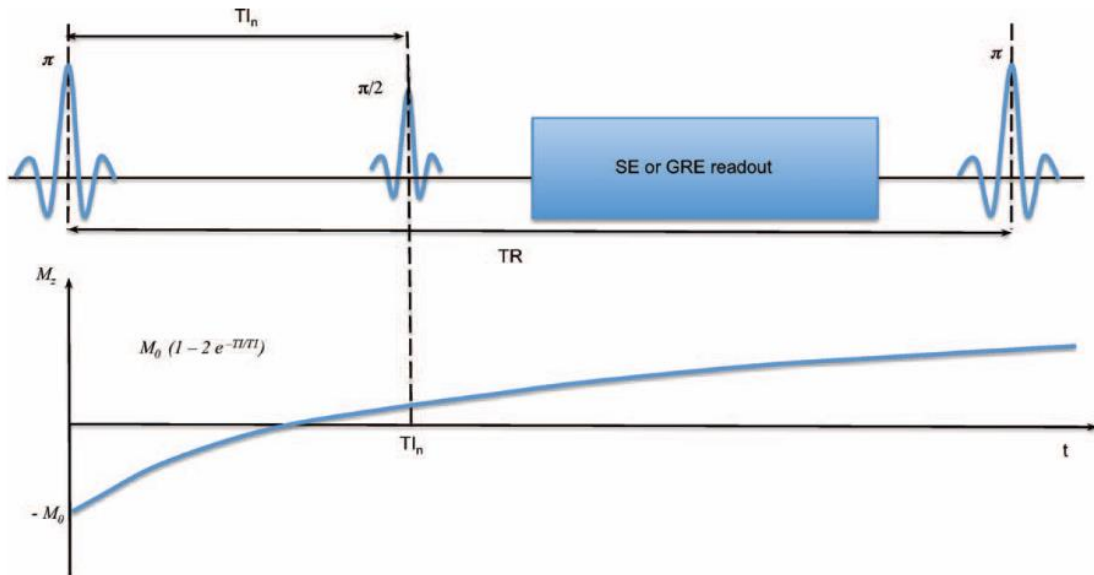


Figure 1: Schematic overview of an IR sequence and the resulting T_1 relaxation curve. The relaxation curve is measured by sampling multiple TI 's. From these TI 's the T_1 can be fitted using the single exponential [61].

2.3.2 T_2 determination

Multi-spin echo (multi-SE) sequences are most frequently used to determine T_2 . With this sequence, multiple echoes are measured during one acquisition. The sequence consists of a 90° pulse followed by a series of 180° pulses, which ideally cover the complete decay of the signal. Each 180° pulse creates an echo which is measured. The number of 180° pulses and, therefore the amount of echoes is called the echo train length (ETL) [27]. Such a sequence to determine the T_2 is called a Carr-Purcell-Meiboom-Gill (CPMG) sequence [28]. To get the T_2 the measured signal of each echo can be fitted with the following equation:

$$S = M_0 \left(e^{-\frac{TE}{T_2}} \right) + a \quad (5)$$

The first measured echo suffers from errors in the refocusing pulse and, therefore should be discarded [27]. Discarding the first echo does not compensate for errors completely; therefore, one should always minimise external field inhomogeneities.

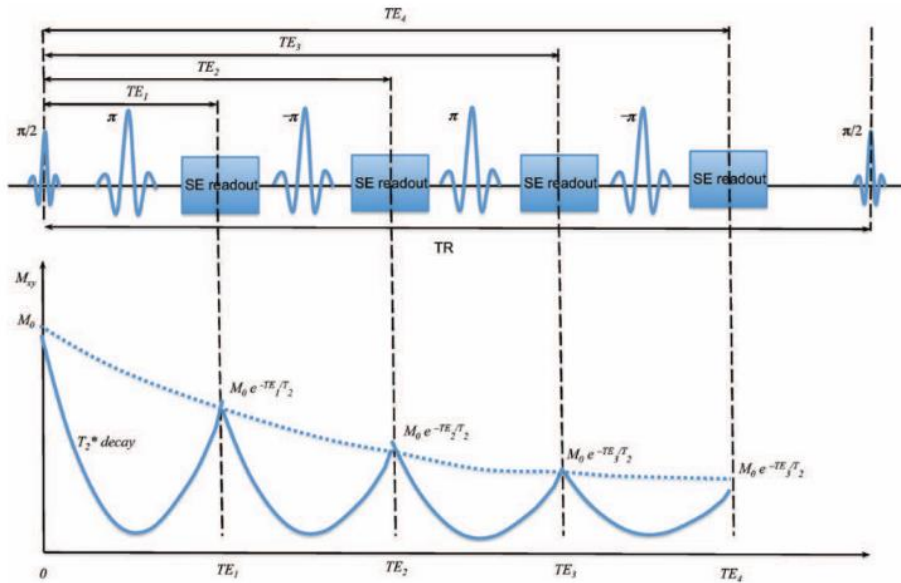


Figure 2: Schematic overview of a multi-SE sequence and the resulting T_2 relaxation curve. The relaxation curve is measured by sampling a train of TE. From these TE's the T_2 can be fitted using the single exponential [61]

2.3.3 Calculation of the relaxivity

The relaxivity of a contrast agent is calculated using the relaxation times determined by the previously mentioned methods of a concentration series of the contrast agent. The number of concentrations in the series increases the accuracy of the relaxivity determination. The optimal number of concentrations in literature is five [29]. After the relaxation times of the concentration series are determined, the relaxivity can be fit. The fit of the relaxivity is done using the following equation, which is derived from equation 3:

$$\frac{1}{T_i} (\text{measured}) = r_i * [C] + a \quad (6)$$

In this equation, a describes the inverse of the initial relaxation time. Figure 1Figure 3 shows an example of a longitudinal relaxivity determination for measurements at 1.5T. On the left, three images, each of a different TI, are shown. A circular region of interest (ROI) is selected from the images. The signal of each ROI is plotted against its TI to create a relaxation curve. T_1 is fitted to this relaxation curve by using equation 4. The inverse of T_1 of different samples is plotted against the concentration of the contrast agent. Whereafter, the relaxivity is fitted using equation 6. For the transversal relaxivity, the process is similar; however, for T_2 determination, equation 5 is used.

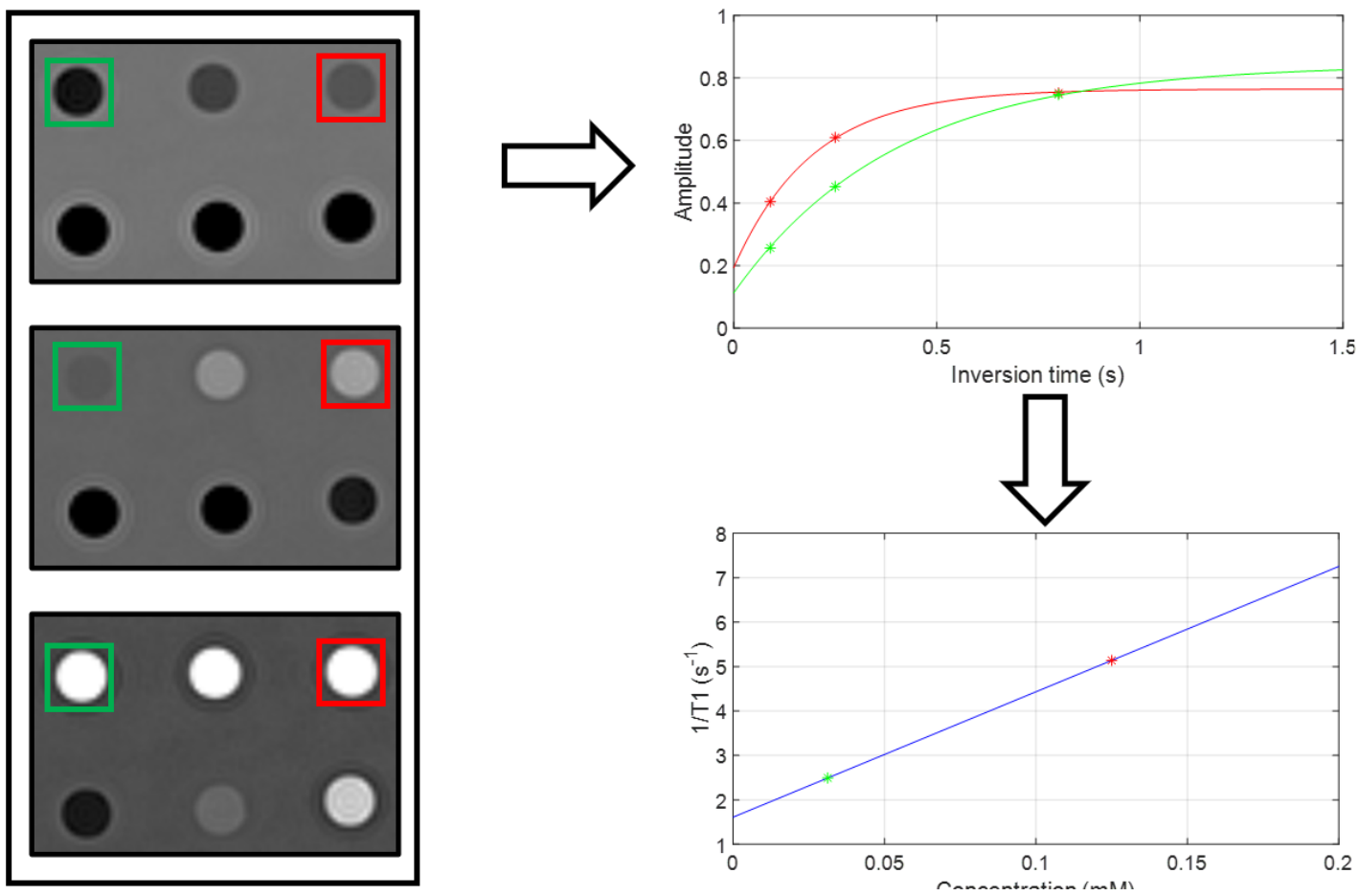


Figure 3: Schematic overview of the procedure to determine the longitudinal relaxivity of a contrast agent. On the left regions of interest are selection from which the signal intensity is plotted again the inversion time to fit T_1 , which can be seen in the top right. By taking the inverse of the measured T_1 and plot it against its contrast agent concentration, the relaxivity slop can be fitted, which can be seen in the bottom right.

3 RELAXIVITY MEASUREMENT STEPS FOR EACH FIELD STRENGTH

The general steps for determining the relaxivity are almost identical for every field strength. First, T_1 and T_2 are measured to determine the relaxivity subsequently. However, the exact steps for measuring T_1 and T_2 can differ between field strengths. This chapter will assess these initial measurement steps to measure the T_1 and T_2 at each field strength. Furthermore, every field strength scanner has its optimal parameter settings, which are considered. Therefore, an investigation for the most optimal parameters for every field strength is described. These parameters include the repetition time (TR), inversion time (TI) and echo time (TE). Lastly, the acquisition settings, like resolution and field of view, are discussed for every field strength.

3.1 MEASUREMENTS AT 0.5T

The 0.5T measurements are performed with a tabletop scanner. The tabletop scanner (Magspec, Pure devices, Germany, see Figure 4) can hold one sample in a tube with a diameter of 15 mm and operates at 37°C to mimic human body conditions. The tabletop can run preprogrammed basic sequences. Parameters in these sequences can be adjusted if necessary.



Figure 4: Picture of the 0.5T tabletop scanner.

3.1.1 Initial measurement steps

To determine T_1 , a preprogrammed script of the tabletop scanner is used. This script determines the T_1 with an IR sequence in OD. For this script, an estimation of T_1 is needed (T_{1e}), which determines the duration of the measurement. The IR sequence measures the signal intensity at several TI's. The TI's are logarithmically divided. The signal intensities measured by the IR sequence are plotted against their TI to get a relaxation curve. To this curve, the T_1 is fitted using a three-parameter non-linear least squares curve fitting algorithm (MATLAB ©2020a©, Mathworks, USA) in combination with equation 4. If the measured T_1 is not in the range of the T_{1e} , then T_{1e} has to be adjusted, and measurements are performed again.

To determine T_2 , a CPMG sequence is used in OD. The CPMG sequence measures the signal decay at a number of TE's. The TE's are plotted against the signal decay to get the relaxation curve of T_2 . T_2 is then fitted to this curve using the same algorithm as for T_1 ; however, equation 5 was used.

After the T_1 and T_2 are determined for every sample, the relaxivities (r_1 and r_2) are determined by the method mentioned in paragraph 2.3.3.

3.1.2 Optimisation steps

For both the T_1 and T_2 measurements, a TR must be set. The TR determines the duration of the T_1 measurement, so optimising this parameter is essential. For T_1 determination, TR must be sufficiently long to include the return of the magnetic signal to the equilibrium state [25]. In a tabletop measurement, the default setting for TR is the T_{1e} multiplied by five. However, a multiplication of four is also found sufficient in literature, reducing the acquisition time by 20% [30]. Therefore, a TR is chosen of four times the T_{1e} . The TR is kept the same for the T_2 measurement.

In the T_1 determination, the number of TI's has to be set. The default number of TI's at the tabletop is 50. A larger number of TI's increases the accuracy of the T_1 measurements and the acquisition time. From literature, 12 TI's are found sufficient to determine the T_1 when logarithmically spread [28]. This spread is applied between a minimal and maximal value of TI. The minimal value is set to the lowest limit of the tabletop, which is 3 ms. The maximal value is set slightly below the TR [30] [25].

For the T_2 determination, a number of TE's has to be set. The measurement duration divided by the echo stepsize determines the number of TE's. The value of TE defines the echo stepsize and starting value. A small echo stepsize will increase the number of TE's if the measurement duration is kept the same. To get the largest number of TE's, and therefore the most data points, the value for TE is set to its lowest limit. This lowest limit result in a TE of 2.3 ms. The measurement duration is set at a length that the whole decay of the MRI signal is measured. If this is not the case, the duration needs to be adjusted.

Besides the TR, TI and TE, other acquisition parameters may be optimised. However, not many of these parameters can be changed for the tabletop scanner. The OD measurements do not allow changes in the field of view (FOV) or resolution-related settings.

3.2 MEASUREMENTS AT 1.5T

The 1.5T measurements are performed using available sequences on a SIEMENS MRI scanner (MAGNETOM Area, SIEMENS, Germany, see Figure 5). Instead of measuring one sample individually, multiple samples can be measured simultaneously. For the 1.5T measurements, a standard head coil is used. The determination of the relaxivities is executed in similar ways as the measurements of the tabletop. However, some changes in the measurement and optimisation steps are outlined in the following sections.



Figure 5: Picture of the 1.5T full body scanner.

3.2.1 Initial measurement steps

A relaxation curve is measured to determine T_1 with the 1.5T scanner. To do so, a standard STIR sequence is used. The STIR sequence is an alteration of the IR sequence. The STIR sequence makes a 2D image for several selected TI. For each TI, an image is reconstructed. The sample's mean signal intensity in each image is determined by evaluating the selected sample's region of interest (ROI). The ROI is determined by drawing a circle around the tube of the selected sample. The signal intensity of this ROI is plotted against its corresponding TI. A relaxation curve is determined when this is done for all the TI. T_1 is obtained by fitting equation 4 to this relaxation curve. Before fitting, the scale of the images is normalised to the maximal and minimal pixel value of the whole image series. The selection of the ROI for each sample has to be done manually.

A standard multi-SE sequence measures the relaxation curve to determine T_2 . The multi-SE sequence makes a 2D image for a number of echoes. Like in the T_1 determination, an ROI is selected, and its signal intensities are plotted against its corresponding TE. Equation 5 is then used to fit T_2 to the plotted relaxation curve.

The relaxivity determination is similar to the tabletop scanner, as mentioned in paragraph 3.1.1.

3.2.2 Optimisation steps

Section 3.1.2 outlines the rationale for most parameters' optimal settings. This includes the TR, TI and TE. The TR for the 1.5T measurements is similar to the tabletop and should be four times T_{1e} . Because samples can be measured simultaneously, this has to be the T_{1e} of the sample with the lowest concentration. The T_2 measurements used the same TR.

The TI's settings differ slightly from the tabletop. Fourteen TI's is used. The TI's are not logarithmically divided because of the higher minimal possible value of the scanner. The minimal value is therefore set at 25 ms. The maximal value of TI is set just below TR. The other TI's are chosen between the minimal and maximal values, with more samples at the shorter times. More TI's are used compared to the tabletop because of the higher minimal value of TI.

The multi-SE sequence uses 32 echoes. The highest accuracy is available with the lowest possible TE; therefore, the TE is set at 14.3 ms. The most important aspect is that the MR signal's decay is sampled completely. Otherwise, a higher TE should be chosen.

The acquisition parameters can be optimised now that the optimal values for TR, TI and TE are chosen. In preliminary experiments, it was found that when using a resolution of 128x128 lines with a FOV of 150x150 mm, Gibbs-ringing occurred. To reduce the Gibbs-ringing, the resolution is increased to 256x256 lines. The FOV is kept at 150x150 mm.

Placing the sample tubes in the 1.5T scanner can be done in multiple ways, like upright or horizontally along the axis of the magnetic field. Due to the changeable slice orientation, a round tube intersection can always be guaranteed. Therefore, the sample tubes are placed upright and measured coronally to keep the setup similar to the tabletop measurements.

3.3 MEASUREMENTS AT 0.25T

The 0.25T measurements are performed using standard protocols on an Esaote MRI scanner (G-scan Brio, Esaote, Italy, see Figure 6). For the 0.25T measurements, a standard knee coil is used. The determination of the relaxivities is executed similarly to the 1.5T scanner. However, there are some changes in the measurement steps, which are mentioned in the next section.



Figure 6: Picture of the 0.25T full body scanner, which is also able to perform upright acquisitions.

3.3.1 Initial measurement steps

Measuring the relaxation curve of T_1 is performed similarly to the 1.5T measurement. A STIR sequence is used, which makes 2D images for several selected TI. However, the range of possible TI is limited for the 0.25T scanner. Furthermore, there are some differences regarding the processing of the signal intensities and the TI to the relaxation curve. The 0.25T scanner uses a different scaling for each 2D image at every TI. Therefore, the whole image series could not be appropriately normalised. To overcome this problem, custom reconstruction was done on the raw data. These reconstructions for each TI could be normalised, and the same processing steps as for 1.5T are followed.

To measure the T_2 relaxation curve, a different sequence than the 1.5T scanner is used. This is needed because the multi-SE sequence is limited on the 0.25T scanner. At the 0.25T scanner, only three echoes can be executed with the multi-SE sequence. Therefore, another way is found to determine the relaxation curve of T_2 . This is done with a self-developed method using an FSE sequence and the raw data.

First, a series of FSE acquisitions is taken with a certain number of echoes, called the echo train length (ETL). For each acquisition, a different effective TE is set, resulting in several FSE acquisitions with different compositions of k-space. These k-spaces of all these acquisitions can be combined and rearranged to get images which consist only of the lines from a single TE. To get an image with only lines of one TE, the place of these lines in all the FSE measurements must be known. The scanner provides this information; therefore, the place of all the lines of a single TE are known in every measurement. All these lines of a single TE are combined to get a k-space with only that TE. This k-space can be reconstructed into a 2D image. This is done for all selected TE to get an image series, which can be normalised and processed to get the signal intensities for every ROI at every TE. These signal intensities can be plotted against their corresponding TE to get the relaxation curve, to which equation 5 can be fitted to get the T_2 .

The relaxivity determination is similar to the tabletop scanner, as mentioned in paragraph 3.1.1.

3.3.2 Optimisation steps

In the optimisation steps described in paragraphs 3.1.2 and 3.2.2, the argumentation is already given for setting the value of TR. The TR is the same for the T_1 and T_2 determination.

TI's are chosen similarly to the 1.5T scanner. However, the smallest possible value of TI is higher, namely 50 ms. There is also a limit to the maximal value of TI, which is 2000 ms.

For the FSE sequence, the ETL and the echo spacing must be optimised. The ETL determines the numbers of TE from which the T_2 is fitted. In paragraph 3.1.1 is stated that the number of TE's has to be as high as possible, with a TE which is as low as possible. For the 0.25T scanner, this results in an ETL of 20 and a TE of 20 ms.

To reduce the Gibbs-ringing, the resolution for the T_1 measurements was set to 192x192 lines. A higher value is possible, but this setting sufficiently reduces the Gibbs-ringing. The T_2 measurements allowed a higher resolution because of the use of the FSE sequence; therefore, the resolution was set to 252x256 mm. The FOV for both relaxation measurements is set to 160x160 mm.

3.4 DISCUSSION

During the development of the protocol of each field strength and by running through the different measuring steps to investigate the optimal parameters, some constraints are found. These constraints are mentioned below.

Only one sample can be measured on the tabletop at once. Therefore if a whole concentration series needs to be scanned, a long time is needed. Multiple samples can be measured simultaneously at the 0.25 and 1.5T scanners, resulting in faster measurements than the tabletop. However, one downside of simultaneously measuring multiple sample concentrations is that the TR has to be based on the T_{1e} of the lowest concentration.

The combination of FSE acquisitions is not ideal because not every TE is k-space fully sampled. This is because the placement of the lines in the FSE acquisitions is not always the same. Nevertheless, show preliminary measurements of the FSE sequence sufficient relaxation curves, to which a T_2 can be fitted.

4 EFFECT OF TEMPERATURE ON RELAXIVITY

The previous chapter described how to determine the relaxivity at each field strength with optimal parameters. Next, this information can be used to define a protocol for SPION measurements. However, in a preliminary investigation of the tabletop scanner's possibilities for measuring olive oil's relaxation time, some issues were found that required attention before SPIONs can be investigated. These issues relate to variabilities in relaxation measurements, where the cause of these variabilities was not clear. In literature, it is found that the cause of these variabilities could be the temperature of the sample [31]. Therefore, to investigate to cause of these variations, the following research question is written:

- Does the temperature of the sample influence the relaxation time and the resulting relaxivity?

A tabletop scanner is used to investigate the influence of the temperature on the longitudinal relaxation time and relaxivity.

4.1 INTRODUCTION

The temperature and stability of the measurements are related, making it hard to define the appropriate settings and the influence of the temperature simultaneously. As stated before, besides the contrast agent, the temperature also influences relaxation times. T_1 increases at higher temperatures [32]. T_2 increases slightly at higher temperatures [31]. However, whether this increase in relaxation times also affects a contrast agent's relaxivities is the question.

4.2 MATERIALS

For performing experiments to answer the research question of this chapter, phantoms are made. These phantoms consist of sample tubes filled with different concentrations of manganese dichloride ($MnCl_2$). $MnCl_2$ is chosen because of its pre-known relaxivity and availability in the lab. Samples tubes were made containing concentrations of 0.07, 0.14, 0.29, 0.58 and 1.15 mM in tap water.

4.3 METHOD

The influence of the temperature is investigated by measuring the T_1 of the $MnCl_2$ concentration series. The T_1 is first measured on the tabletop without pre-heating at room temperature ($\sim 21^\circ$). After that, the samples are placed in a water bath of $37^\circ C$ for at least one hour. Then relaxation times are measured again on the tabletop. Before and after the measurements, the temperature of the samples is measured during measurements without pre-heating. The method for the T_1 measurements is given in the previous chapter. The protocol used can be found in Appendix A.2.

4.4 RESULTS

Table 1 shows the results of the temperature test. For every concentration, the T_1 increases at a higher temperature. The percentual difference between the T_1 at room temperature and 37°C is around 15.6 ± 1.5 %. The scan time of the samples decreased with increasing sample concentration due to the lower T_1 . Furthermore, Table 1 shows that the variable 'Temp change' increases with increasing scan time. From this, it can be deduced that the tabletop warms up the samples during the measurements.

Table 1: Results of the temperature measurements from the tabletop scanner. For every concentration are, the measurements performed separately.

Concentration (mM)	0.07	0.14	0.29	0.58	1.15
Scan time (s)	370	269	181	133	116
Temp start (°C)	21.2	20.5	20.7	21.1	21.3
Temp end (°C)	27.6	26.0	25.3	24.5	23.8
Temp change (°C)	6.4	5.5	4.4	3.4	2.5
T_1 Room temp (ms)	1283	845	540	315	185
T_1 37°C (ms)	1494	1012	642	372	220
T_1 difference (ms)	211	167	102	57	35
Percentual difference	14.1 %	16.5 %	15.9 %	15.3 %	15.9 %

Figure 7 shows the determined relaxivity slopes. The relaxivity at room temperature (around 21°) is shown in blue, and red shows the relaxivity at 37°C. The respective relaxivities are 4.22 and 3.57 $\text{mM}^{-1}\text{s}^{-1}$. Both slopes had the same adjusted R^2 of 0.977.

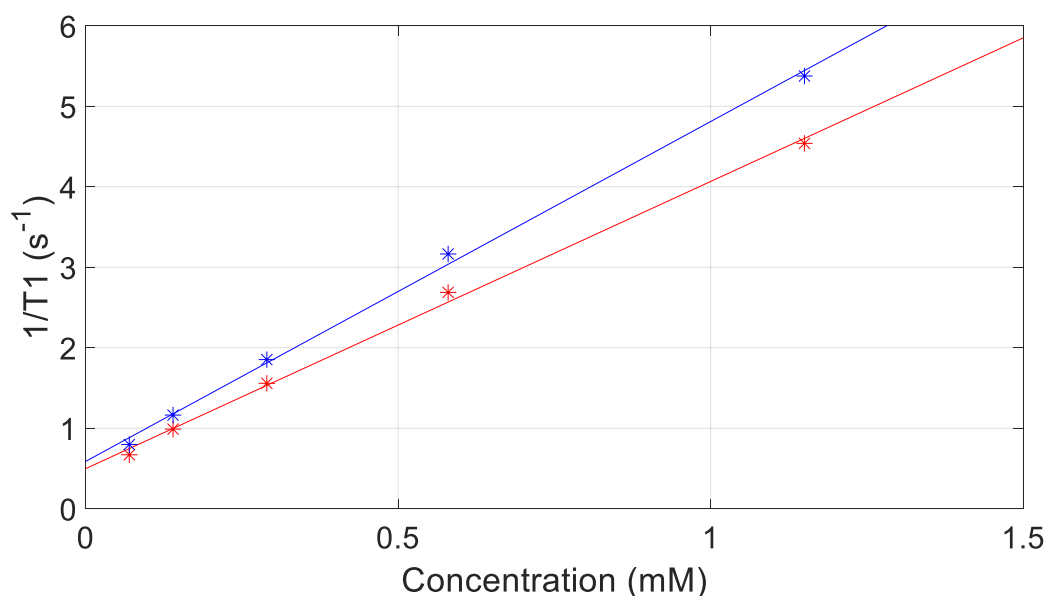


Figure 7: Determined relaxivities of MnCl_2 concentration series without pre-heating (blue) and with pre-heating (red). The respective relaxivities are 4.22 and 3.57 $\text{mM}^{-1}\text{s}^{-1}$.

4.5 DISCUSSION

The performed experiments in this chapter aim to assess the importance of measuring the longitudinal relaxivity at a clinically relevant temperature of 37°C. The results are consistent with another study stating that T_1 increases with increasing temperature [33][34].

The most important finding is that the longitudinal relaxivity is temperature-dependent. A higher temperature results in lower relaxivity, shown in Figure 7. This means that the value of T_1 and the amount of change in T_1 is temperature-dependent. This result indicates that contrast agents are less effective at higher temperatures, resulting in a relaxivity overestimation when contrast agents are measured at lower temperatures than 37°C.

Another interesting finding is that the increase of T_1 due to temperature depends on the initial magnitude of T_1 . At similar temperature changes, a more significant increase in magnitude for samples with long T_1 than with a short T_1 is found, indicating that the initial magnitude influences the total increase of T_1 . This dependency looks constant with a percental difference of around 15 % between room temperature and 37°C. This 15 % difference is also applicable for the determined relaxivity and would give higher variations in higher relaxivity materials, emphasising the need to measure at a constant temperature.

One important finding found during the execution of the measurement is the heating of samples during the measurement. This influences the T_1 determination and possibly the variabilities mentioned in the introduction of this chapter. Therefore, it is crucial to ensure that samples are adequately pre-heated to a temperature of 37°C.

The influence of temperature on transversal relaxivity is not investigated. However, literature shows that this relation is less significant and therefore is chosen not to investigate this [35].

4.6 CONCLUSION

The results clearly show that the temperature affects the relaxation time and relaxivity. The results also show that samples without pre-heating warm up in the tabletop scanner. A difference can be seen in temperature before and after the measurements. This means that the tabletop induced heat to the sample. Therefore, all following measurements have to pre-heat the sample in a water bath at 37°C. This study shows that, for measuring the relaxivities of contrast agents comparable to in vivo studies, measurements must be performed at 37°C. Otherwise, the relaxivity is overestimated.

5 SPION RELAXIVITY MEASUREMENTS AT EACH FIELD STRENGTH

In this chapter, the SPION relaxivity measurements are described. First, the fabrication of the SPION concentration series is discussed in the materials section. This involves the selection of three different SPIONs and the fabrication of a concentration series of these SPIONs. After that, the different relaxivity measurements are discussed regarding protocol specifications, scanning parameters, temperature regulation and scanning procedure in the method section.

5.1 MATERIALS

5.1.1 SPION selection for relaxivity measurements

SPIONs come in a large variety of sizes, different types of coating and different iron content. This research intends to get an insight into SPION relaxivity on low-field. Therefore, three SPIONs were chosen, available at the research group. The selection of the SPIONs is based on the size of the SPIONs. Chapter 3 states that a smaller size increases the relaxivity ratio (r_1/r_2) and could lead to positive contrast. Therefore, three SPIONs are chosen with the smallest size available. The smallest SPION is EMG304 (FerroTec Corporation, USA), with a diameter of 10 nm. EMG304 is soluble in water and consists of 4.5 % of the iron oxide particle magnetite, resulting in an iron concentration of 0.723 M. The second chosen SPION with a diameter of 25 nm is SPH25 (Ocean Nanotech, USA). SPH25 is a carboxyl iron oxide nanoparticle with an iron content of 5 mg/ml, which results in an iron concentration of 0.0895 M. The last chosen SPION is SynomagD50 (micro mod, Germany) which has a diameter of 50 nm. SynomagD50 is a dextran iron oxide composite particle with an iron content of 10 mg/ml, which results in an iron concentration of 0.179 M.

5.1.2 Dilution medium

The SPIONs must be diluted in a clinically relevant medium to determine a clinically relevant relaxivity. When the SPIONs are used as contrast agents, they change blood relaxivity, not water. Therefore, it is crucial to perform the relaxivity measurements in blood. The availability of human blood is scarce, and ethical applications need to be done to use it in the study. Therefore, it is chosen to use porcine blood. This is similar to human blood's composition and protein content [36] and is easily available.

The collection of blood and consecutive tests need to be done as soon as possible after slaughter. This is important because the T_1 and T_2 of blood will change over time [37]. Heparin is added to keep the blood from clotting. Adding heparin to blood is common in relaxivity research [17]. Heparin is an anticoagulant used to decrease blood clotting, which could also influence relaxation times.

5.1.3 SPION sample fabrication

Because of the limitation of the 0.25T scanner, a range of desired T_1 times is set. This range is set between 250 ms and 500 ms because of the TI limits of the 0.25T scanner. A preliminary test is performed to fabricate SPION concentrations that generate these relaxation times. The results of the preliminary test are given in Appendix B.

In this preliminary test, the following longitudinal relaxivity values were found for the SPIONs: 12.15 $\text{mM}^{-1}\text{s}^{-1}$ for EMG304, 10.56 $\text{mM}^{-1}\text{s}^{-1}$ for SPH25 and 38.95 $\text{mM}^{-1}\text{s}^{-1}$ for SynomagD50.

To calculate the SPION concentrations, equation 3 was rewritten to:

$$[C] = \frac{\left(\frac{1}{T_1(C)} - \frac{1}{T_1(0)}\right)}{r_1} \quad (7)$$

When 250 ms and 500 ms are used as the highest and lowest $T_1(C)$, a range of concentrations can be calculated when $T_1(0)$ is known. $T_1(0)$ of porcine blood at 37°C was measured to be around 1 s. The calculated concentration is given in Table 2.

Table 2: Calculated concentration of each SPION to keep the T_1 in the range of the 0.25T limit.

$\sim T_1$ (ms)	EMG304 (mM)	SPH25 (mM)	SynomagD50 (mM)
500	0.0205	0.125	0.011
400	0.0308	0.168	0.028
333	0.0410	0.218	0.045
285	0.0515	0.266	0.062
250	0.0618	0.313	0.079

5.2 METHOD

5.2.1 Protocol specifications

For the measurements of the SPIONs, the same steps are followed, as mentioned in chapter 3 and described in Appendix A. However, some adjustments are needed. Because of the use of blood, some actions are added to the protocol. These actions include the in-between agitating of the blood samples during the measurements. This agitation has to be done before every measurement at 0.5T and every ten minutes for the 0.25T and 1.5T measurements. Because of the agitations, the sample tubes could change position; therefore, a new ROI must be selected with every agitation. The agitating needs to be done to prevent the sedimentation of the red blood cells in the blood. Another way to reduce this sedimentation is by measuring the sample tube upright.

5.2.2 Scanning parameters

With the calculated concentrations, there is already an estimated T_1 of every SPION concentration. In Table 3, the resulting parameters of each scanner are given. These parameters are based on the optimisation steps in paragraphs 3.1.2, 3.2.2 and 3.3.2.

Table 3: Parameter settings of the three scanners during the different SPION measurements. * The TE was changed after the measurements of the SPION SPH25 to increase the number of data points. For the SPH25 measurements, the TE ranged from 30 to 600 ms at 0.25. The echo train at 1.5T started at 15 ms.

	Field strength	Sequence	TR (ms)	TE (ms)	TI (ms)	Voxel size (mm)
T_1	0.25T	IR	2000	80	50,100 150, 200, 250, 300,350, 500, 750, 1000, 1500 & 1850	0.78x0.78x5.0
	0.5T	IR	4 x estimated T_1	-	3 to TR, increased logarithmically	15.0x15.0x15.0
	1.5T	IR	2000	8.3	25,50,100 150, 200, 250, 300,350, 500, 750, 1000, 1250, 1500 & 1950	0.59x0.59x5.0
T_2	Field strength	Sequence	TR (ms)	ETL	TE (ms)	Voxel size (mm)
	0.25T	FSE	2000	20	20 up to 400*	0.63x0.63x5.0
	0.5T	Multi SE	4 x estimated T_1	500	2.3 up to 2000	15.0x15.0x15.0
	1.5T	Multi SE	2000	32	14.3 up to 457.6*	0.59x0.59x5.0

5.2.3 Temperature regulation

The measurements described in chapter 4, with the tabletop scanner, made it apparent how important the temperature is in the T_1 measurements and the calculation of the relaxivity. A heat regulation setup has been homemade to ensure a similar temperature as the tabletop measurements for better comparability and clinical relevancy. This heat regulation setup consists of an isolated box wherein the sample tubes can be placed. Inside this box is a pipe system connected to a warming system (Variotherm 550, Hico medical systems, Germany). Figure 8 shows a picture of the isolated box with the pipe system. The warming system pumps 39°C water through the pipe system, resulting in a temperature of 37°C inside the box. At the start of every measurement, the box is filled with water at 37°C. Before placing samples into the heat regulation system, they are pre-heated in a water bath at 37°C for at least one hour.



Figure 8: Picture of the isolated box used in the heat regulation setup. Through the internal pipesystem 39°C water is run through which keeps the water inside the box at 37°C. Samples tubes can be placed inside the yellow brackets.

Because of the water flow in the heat regulation setup, flow artefacts can occur during the 0.25 and 1.5T measurements. To ensure that these flow artefacts do not hinder the measurements, the phase encoding direction had to be set so that the flow artefact does not interfere with the signal of the sample tubes.

At the 0.25T scanner, the samples tube and the heat regulation system could not fit upright in the knee coil. To maintain the upright position of the tube, one option could be to switch to a bigger coil. However, this would reduce the measurements' signal-to-noise ratio (SNR). Luckily, it is possible to rotate the MRI table of the 0.25T scanner so that the sample tubes are imaged upright inside the knee coil.

5.2.4 Scanning procedure

Because of the change in T_1 and T_2 of blood over time mentioned in paragraph 5.1.2, it is crucial to work fast. Therefore a structured procedure is written to measure the relaxivity of SPIONs in blood, which is given below:

When the fresh blood arrives at the lab, a concentration series of the selected SPION is made directly in sample tubes. The tubes are then placed in a water bath of 37°C. After at least one hour, the tubes can be measured on the tabletop scanner. When the measurements of one sample are completed, it is placed back in the water bath so that all the samples have been in the water bath for the same time. When all samples have been measured, the samples go into the refrigerator. The next day, the samples are warmed up in the water bath and then measured in the 1.5T and the 0.25T scanner. After all measurements are done, they can be processed. When the samples are found to be out of the 0.25T scanner range during the measurements of the tabletop scanner, a new concentration series must be made.

5.3 RESULTS

In this section, the results of relaxivity measurements are described. Every SPION is discussed separately. With measured longitudinal and transversal relaxivity, relaxivity ratios are calculated.

5.3.1 EMG304

5.3.1.1 Longitudinal relaxivity

Figure 9 shows the results of the longitudinal relaxivity (r_1) measurement of EMG304 at every field strength. For EMG304 longitudinal relaxivities were found of 19.84 $\text{mM}^{-1}\text{s}^{-1}$ at 0.25T, 65.31 $\text{mM}^{-1}\text{s}^{-1}$ at 0.5T and 9.68 $\text{mM}^{-1}\text{s}^{-1}$ at 1.5T. Noticeably, the lower adjusted R^2 for the 0.25T measurement can also be seen at the bad fit of the lowest and highest concentration.

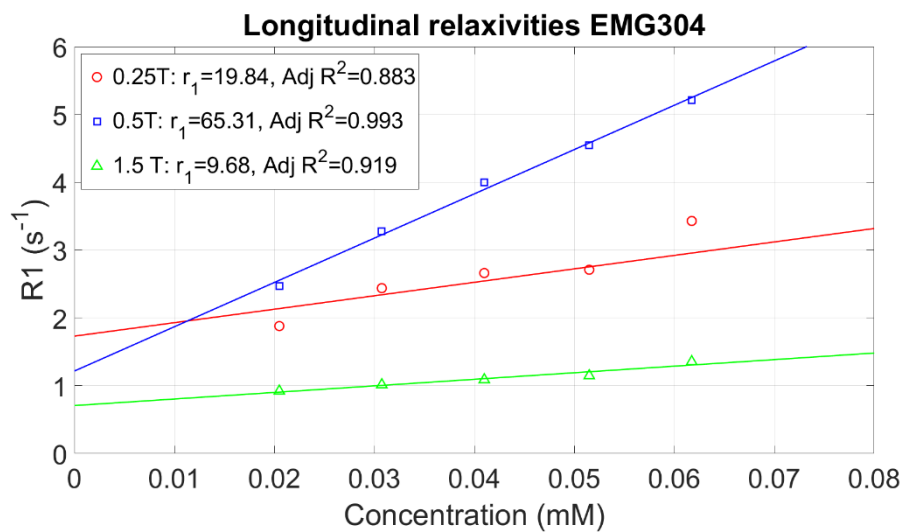


Figure 9: Longitudinal relaxivities of EMG304 at 0.25, 0.5 and 1.5T. Adjusted R^2 is given to indicate the goodness of the fit of the relaxivity.

5.3.1.2 Transverse relaxivity

Figure 10 shows the results of the transverse relaxivity (r_2) measurement of EMG304 at every field strength. For EMG304 transverse relaxivities were found of 249.65 $\text{mM}^{-1}\text{s}^{-1}$ at 0.25T, 429.02 $\text{mM}^{-1}\text{s}^{-1}$ at 0.5T and 175.05 $\text{mM}^{-1}\text{s}^{-1}$ at 1.5T. For every field strength, the adjusted R^2 is above 0.947.

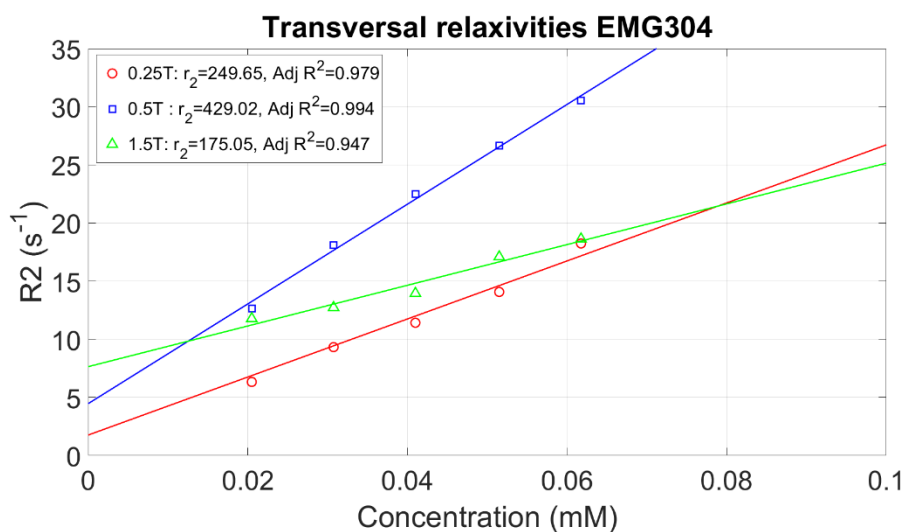


Figure 10: Transverse relaxivities of EMG304 at 0.25, 0.5 and 1.5T. Adjusted R^2 is given to indicate the goodness of the fit of the relaxivity.

5.3.2 SPH25

5.3.2.1 Longitudinal relaxivity

Figure 11 shows the results of the longitudinal relaxivity (r_1) measurement of SPH25 at every field strength. For SPH25, longitudinal relaxivities were found of $18.09 \text{ mM}^{-1}\text{s}^{-1}$ at 0.25T, $13.55 \text{ mM}^{-1}\text{s}^{-1}$ at 0.5T and $2.58 \text{ mM}^{-1}\text{s}^{-1}$ at 1.5T. Noticeable is the low adjusted R^2 for the 0.25T measurement. Therefore, it is essential to bear in mind the possible bias in the determined relaxivity.

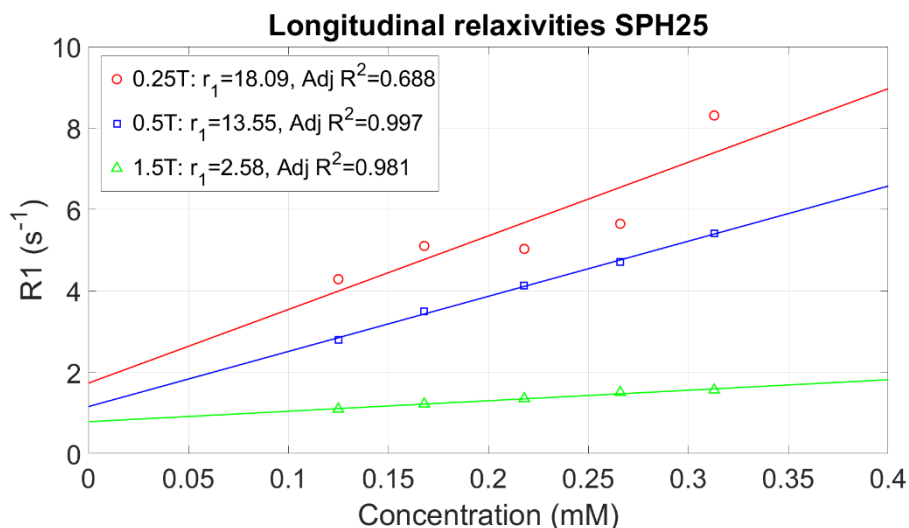


Figure 11: Longitudinal relaxivities of SPH25 at 0.25, 0.5 and 1.5T. Adjusted R^2 is given to indicate the goodness of the fit of the relaxivity

5.3.2.2 Transverse relaxivity

Figure 12 shows the results of the transverse relaxivity (r_2) measurement of SPH25 at every field strength. For SPH25 transverse relaxivities were found of $66.94 \text{ mM}^{-1}\text{s}^{-1}$ at 0.25T, $99.66 \text{ mM}^{-1}\text{s}^{-1}$ at 0.5T and $58.03 \text{ mM}^{-1}\text{s}^{-1}$ at 1.5T. Noticeably, the very low adjusted R^2 for the 0.25T measurement results in a biased fit of the transversal relaxivity.

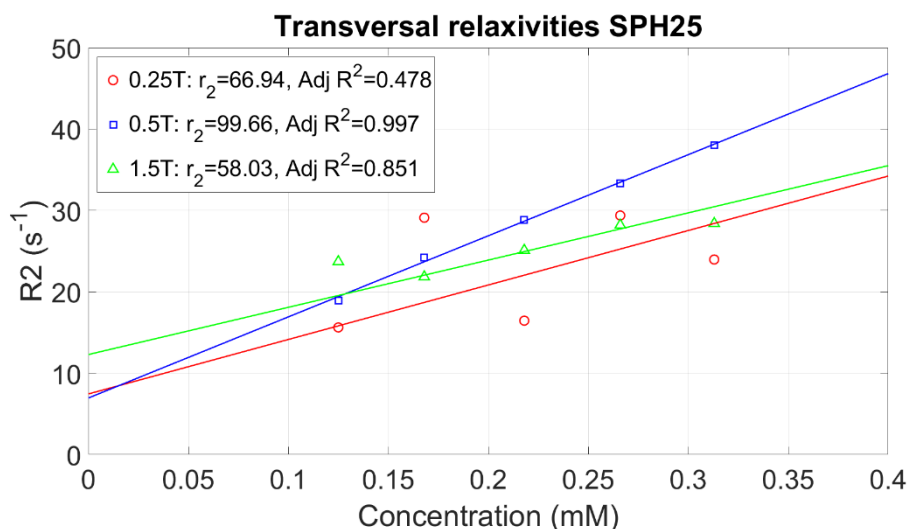


Figure 12: Transverse relaxivities of SPH25 at 0.25, 0.5 and 1.5T. Adjusted R^2 is given to indicate the goodness of the fit of the relaxivity

5.3.3 SynomagD50

5.3.3.1 Longitudinal relaxivity

Figure 13 shows the results of the longitudinal relaxivity (r_1) measurement of SynomagD50 at every field strength. For SynomagD50 longitudinal relaxivities were found of 47.20 $\text{mM}^{-1}\text{s}^{-1}$ at 0.25T, 43.44 $\text{mM}^{-1}\text{s}^{-1}$ at 0.5T and 5.52 $\text{mM}^{-1}\text{s}^{-1}$ at 1.5T. For every field strength, the adjusted R^2 is above 0.933.

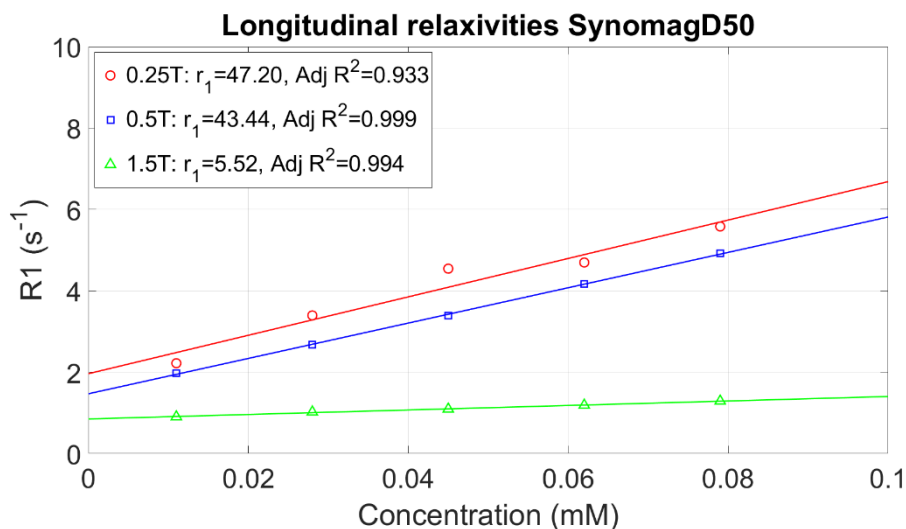


Figure 13: Longitudinal relaxivities of SynomagD50 at 0.25, 0.5 and 1.5T. Adjusted R^2 is given to indicate the goodness of the fit of the relaxivity

5.3.3.2 Transverse relaxivity

Figure 14 shows the results of the transverse relaxivity (r_2) measurement of SynomagD50 at every field strength. For SynomagD50 transverse relaxivities were found of 212.02 $\text{mM}^{-1}\text{s}^{-1}$ at 0.25T, 283.25 $\text{mM}^{-1}\text{s}^{-1}$ at 0.5T and 126.05 $\text{mM}^{-1}\text{s}^{-1}$ at 1.5T. For every field strength, the adjusted R^2 is above 0.978.

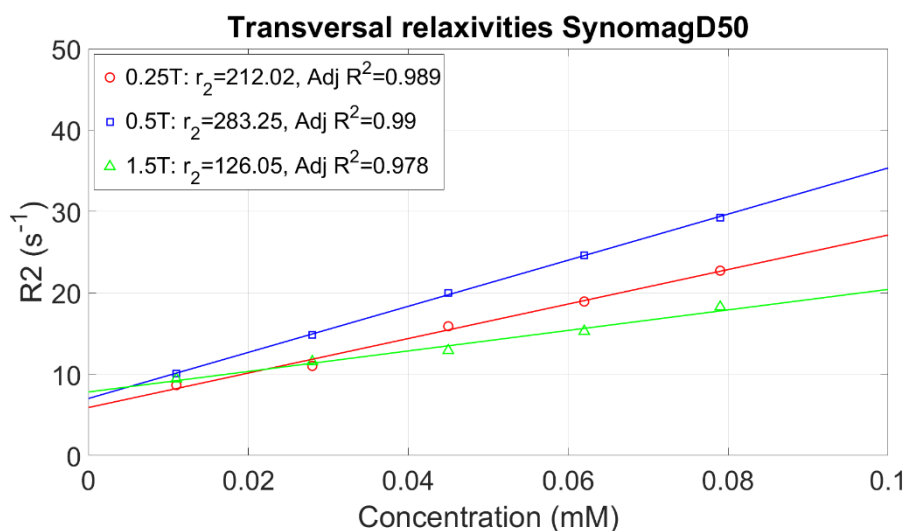


Figure 14: Transverse relaxivities of SynomagD50 at 0.25, 0.5 and 1.5T. Adjusted R^2 is given to indicate the goodness of the fit of the relaxivity

5.3.4 Relaxivity ratios

The relaxivity ratio for every SPION is calculated using the measured relaxivities. These ratios are shown in Table 4. Besides the measured SPION ratio, a gadolinium-based contrast agent (Dotarem) is also added from literature. A high ratio is more favourable for positive contrast. For every SPION, the ratio is below 0.06 at 1.5T, resulting in negative contrast. At low-field strengths, this ratio is higher, with a maximum of 0.222 for SynomagD50 at 0.25T. Although the relaxivity ratio of Dotarem is more than ten times higher at 1.5T, it is lower at 0.25T when compared with the SPIONs. The relaxivity ratio for the SPION SPH25 is not shown. It is decided not to use the SPH25 relaxivity measurements due to the low adjusted R².

Table 4: Calculated relaxivity ratio (r_1/r_2) for each SPION. Values for Dotarem were extracted from literature. The relaxivity ratio of all SPIONs increases from high- to low-field, which makes them beneficial for positive contrast.

		EMG304	SPH25	SynomagD50	Dotarem
0.25T	r_1/r_2	0.079	-	0.222	0.166 [8]
0.5T		0.152	0.136	0.153	-
1.5T		0.055	0.044	0.044	0.627 [17]

5.4 DISCUSSION

In this section are the results of each SPION discussed. With this, the surprising outcomes are explained. Lastly, the calculated relaxivity ratios are discussed, and the strong and weak points of the measurements are stated.

5.4.1 EMG304

What is surprising about the results of the longitudinal relaxivities of EMG304 is that the highest longitudinal relaxivity is found at a field strength of 0.5T, shown in Figure 9. Work by P. Caravan et al. [38] suggests that a low-field strength would result in higher relaxivity, and therefore the highest relaxivity would be expected at a field strength of 0.25T. In another study, the maximal longitudinal relaxivity of a SPION was found at a field strength of 0.1T [19]. This study does not show this behaviour. A possible alternative explanation of this finding is that the relaxivity of this SPION is at a maximum at a field strength of 0.5T. This maximum depends on the composition of the SPION or contrast agents [17]. However, more relaxivity values must be determined at other field strengths to back this statement. An error in one or both of the relaxivity measurements might also be a possible explanation. It could be that the measurement at 0.5T is executed in such a way that it resulted in a higher relaxivity or that the measurement at 0.25T is performed in such a manner that it resulted in a lower relaxivity. Furthermore, has the fit of the 0.25T measurements a lower adjusted R², indicating a worse fit than the other two measurements. An explanation of the worse fit at 0.25T is not found in a mis fabrication of the concentration series because the measurement at the other field strength shows high adjusted R², assuming the correct fabrication of the concentration series.

Surprisingly, the transversal relaxivity of the 0.5T measurements is also the highest for all field strengths. This finding contrasts previous studies, which have suggested that transversal relaxivity decreases with increasing field strengths [16] [37]. It is difficult to explain this result, but it might be related to the short echo time used in the 0.5T measurements. A shorter echo time with shorter echo spacing results in a higher signal in the relaxation measurements, which could result in higher relaxivities. However, it is not clear if the contribution of shorter echo times is solemnly the reason for the increase in transversal relaxivity. Nevertheless, does the measurement show an adjusted R² of 0.94 or higher, which indicates well-fitted slopes.

5.4.2 SPH25

The measured longitudinal relaxivities of SPH25, shown in Figure 11, agree with previous research regarding the increase in relaxivity with decreasing field strength [38]. However, a note of caution is due here since the goodness of the relaxivity fit, represented by the adjusted R^2 , of the highest relaxivity at 0.25T is very low, only 0.688. The reason for this is unclear, but it may have something to do with an error during the 0.25T measurement, which did not occur in the measurements of the other scanners. When looking at the initial T_1 measurements, the goodness of fits is presented with adjusted R^2 above 0.998, indicating correct measurements. Although the order of the relaxivity is in agreement with literature, results should be interpreted cautiously.

Figure 12 shows the measured transversal relaxivities of SPH25 at 0.25T, and one finding that stands out is the low adjusted R^2 of 0.478. This means that the fit can explain less than 50% of variance, so the resulting relaxivity can not be considered for further processing. A possible explanation might be that fewer data points were used for 0.25T measurement compared with the other field strengths. A smaller amount of data points results in a T_2 estimation which is less accurate. However, the goodness of fit in this T_2 estimation was given by an adjusted R_2 with a value above 0.928, representing reasonable accurate measurements.

The order of transversal relaxivities is equal to that of the previous SPION, with the highest relaxivity found at a field strength of 0.5T. Similar argumentation holds for this SPH25, with the addition that transversal relaxivity at 0.25T has not to be taken into account due to the worse fit.

5.4.3 SynomagD50

The longitudinal relaxivity measurement of SynomagD50 shows high goodness of fit represented by a minimal adjusted R^2 of 0.933 for all field strength. Furthermore, there is an increase in relaxivity for decreasing field strength, which accords with the observations for the measurements with the SPION SPH25, which is also found in previous work [38].

The transversal relaxivity measurements show similar goodness of fit as the longitudinal relaxivity measurements, with a minimal adjusted R^2 of 0.978 for all field strengths. However, the order of the relaxivity shows the same behaviour as the other SPIONS, where the 0.5T measurement shows the highest relaxivity. This finding differs from other research, where the lowest field strength results in the highest relaxivity [17], [39]. One explanation could be the different TE used in the transversal relaxation curve determination. For all relaxivity measurements, a TE is chosen as small as possible to reduce the effect of diffusion [40]. However, the 0.5T measurement at the tabletop had a TE of 6.2 times shorter than the 1.5T measurements and 8.7 times shorter than the 0.25T measurements. This much shorter TE could have caused the seen increase in transversal relaxivities. For further research, keeping the TE of the different field strength in the same range, between 14 and 20 ms would be advised. In this way still enough points are samples to determine the transversal relaxation and the effect of diffusion is kept approximate equal.

Lastly, during the measurements at 0.25T and 1.5T, the signal's decay behaved strangely at some TE. This resulted in a sudden increase and decrease of the signal intensities, after which the signal followed the T_2 decay again. A short literature search was performed to investigate the cause of these changes. The research found that the cause of this are stimulated echoes [41]. Stimulated echoes are caused by RF-pulse imperfections, which produce additional echoes at a different TE [42]. Methods for compensation for stimulated echoes are developed but cannot be used retrospectively. However, to decrease the influence of the stimulated echo, it is allowed to correct these signals [43].

5.4.4 Relaxivity ratios

The present study was designed to determine the possibility of SPIONs as a positive contrast agent at low-field MRA. The relaxivity ratio is determined, which indicates the favourability of positive contrast. In Table 3 are the relaxivity ratios given for all the measurements. The ratios show the capability of the SPION SynomagD50 at low-field because of the higher ratio compared with Dotarem. However, the SPION EMG304 shows a lower ratio than Dotarem at 0.25T.

Besides the higher longitudinal relaxivity, the most interesting finding is that the SPION with the biggest core diameter, SynomagD50, has the highest relaxivity ratio and, therefore, is the most favourable for positive contrast. This finding is somewhat surprising given that other studies show higher relaxivities for SPIONs with decreasing core sizes [44]. This conflicting experimental result could be associated with a difference in the coating of the SPIONs. One SPION was coated with dextran (SynomagD50), one with carbonyl (SPH25), and the other (EMG304) did not mention any coating. It is possible that the coating has more influence on the relaxivity than expected. Some research has been found addressing these influences [45]. However, more comprehensive and controlled studies are needed to reveal the complexity of interactions involved in the relaxivity of SPIONs.

Furthermore, because of the small sample size of only three SPIONs, caution must be applied, as the finding might merely reflect a selection effect. If other SPIONs were selected, then maybe other results could be found. Nevertheless, the results show favourable relaxivity ratios on low-field. Whether results are favourable due to size or coating needs further investigation.

The results show a favourable relaxivity ratio for positive contrasts. Statements on whether the specific relaxivity ratio is sufficient are hard to do. Literature describes some boundaries, but these studies do not give a hard boundary. Rather, the relaxivity ratio of the now-used contrast agents is generalised. T_1 contrast agents have high ratios between 0.5 and 1, and T_2 contrast agents show ratios below 0.1. [22]. To reach these ratios, the longitudinal relaxivity needs to be as high as possible and the transversal relaxivity as low as possible, which is an open challenge in developing positive contrast SPIONs.

5.5 CONCLUSION

This investigation's results show that the relaxivity ratio of SPIONs is higher at 0.25T and 0.5T compared to 1.5T. An implication of this is the possibility of the SPION SynomagD50 creating positive contrast at 0.25T due to its relaxivity ratio of 0.220. Figure 15 shows an image of SynomagD50 where the positive contrast can be seen at a particular concentration. The results of SynomagD50 further support the capability of SPIONs at low-field and show high goodness of fit for both r_1 and r_2 . Whilst the results did not confirm the dependency of SPIONs size on the relaxivity, they partially substantiated the importance of the size and coating of the SPION concerning the relaxivity ratio. Although the results have successfully demonstrated that SPIONs have higher relaxivity ratios at low-field, it has certain limitations regarding the respective relaxivities.

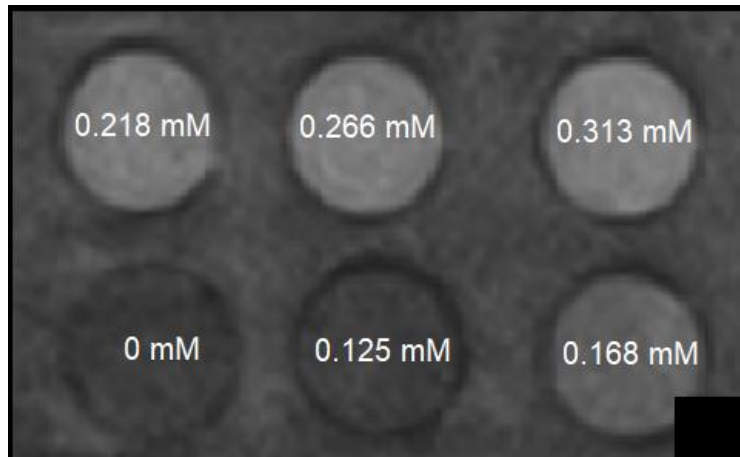


Figure 15: An IR acquisition of the SynomagD50 showing positive contrast at a concentration of 0.168 mM. This acquisition is measured at the 0.25T scanner.

6 GENERAL DISCUSSION

This chapter includes a discussion of the whole report. Every other chapter is discussed shortly, and discussion points are outlined. The chapters in which already a discussion was mentioned are only shortly gone over. Lastly are the recommendations given for further work and further research.

6.1 BACKGROUND

This study aimed to assess the possibility of SPIONs as positive contrast agents in low-field MRA. In reviewing the literature, a theoretical background was described for the methodology to determine the T_1 and T_2 . For determining T_1 , an IR sequence is used. However, faster methods are possible. A faster measurement would assist the downside of using blood in the measurement and could be more favourable. However, the method chosen in this research is the most reliable and robust method to determine T_1 [46].

When looking at equation 6 to calculate the relaxivity, it seems there is no dependency on the medium where the contrast agents are dissolved in. Only the r_1 and the concentration determine the effect the contrast agent will have on the initial relaxation time of the medium. However, literature shows that the medium also affects the contrast agent's efficiency [47]. This is because the accessibility of the protons and their tumbling rate depend on the medium's type and composition. This means that measurements which give a relaxivity in water do not represent the relaxivity of the contrast agent in blood and do not contribute to clinically relevant research.

6.2 TEMPERATURE MEASUREMENT

The investigation of the influence of temperature on the longitudinal relaxivity emphasised the need to measure at a clinically relevant temperature of 37°C. It is important to bear in mind the possible bias in relaxivity research which was not executed at this clinically relevant temperature. A lower temperature will result in higher relaxivities. Therefore the efficiency of contrast agents measured in such conditions can be overestimated.

6.3 PROTOCOL DEVELOPMENT

An initial objective of this research was to develop a robust and accurate protocol to determine the relaxivities of SPIONs. A different protocol is used for each field strength to determine the relaxivities. These protocols are based on the inversion recovery sequence for the longitudinal determination and a multi-SE sequence for the transversal determination. The actual protocol for each field strength differs due to the limitations and possibilities of each scanner. For the field strengths of 0.5 and 1.5T, preprogrammed sequences could be used, from which the relaxation curve could be determined to calculate the relaxivities. However, this was not possible at the scanner with a field strength of 0.25T; therefore, alterations to available sequences needed to be made. This resulted in custom imaging schemes to determine the longitudinal and transversal relaxation curves. Using the multiple FSE acquisitions to determine the transversal relaxation curve is an innovative way to overcome the unavailability of a multi-SE sequence. Despite not sampling the whole of k-space in the FSE measurements, do the results show good adjusted R^2 for the relaxivity measured of EMG304 and SynomagD50. Only the SPH25 measurement showed low adjusted R^2 , resulting in discarding the SPION for further calculation of the relaxivity ratio. Besides that, no other research has been found that also uses this method for the determination of transversal relaxation, making a new method for transversal relaxation determination at the Esaote scanner at the University of Twente.

The present research was designed to compare the relaxivity of SPIONs at three different field strengths. However, the question remains whether it is justified to compare the results of each field strength while the scanning parameters for each field strength were different. The different TE at the T_2 measurements could be a reason for the surprising order of transversal relaxivities. Besides the TE, the TR differed between the 0.5T and other measurements. However, a sufficient long TR of four times T_1 is used for all measurements, making the results comparable [30]. Although the parameters differ per field strength, they were optimised for the respective field strength, resulting in the most accurate way to measure each field strength. Since the differences in parameters only ensured the most accurate measurement possible, it is argued that the measured relaxivities of each field strength can be compared with each other.

6.4 SPION & SAMPLE SELECTION

The measurements in this research are conducted in clinically relevant conditions, e.g. at 37°C and in blood. However, many studies do not use blood. Other fluids like water, plasma or PBS are used instead of blood. This does not give a good representation of how contrast agents behave inside the human body. Blood contains multiple proteins that can influence the contrast agents' relaxivity [47][48]. However, there is also a downside to using blood. Firstly, the experiments need to be executed as soon as possible after the blood extraction because the initial relaxation time of blood changes over time [37]. This gives only a short time window in which the experiments can be planned and give little room for mistakes. Furthermore, blood sediments over time and must be agitated during experiments to keep a homogeneous solution. Nevertheless, if these disadvantages are considered, clinically relevant measurements can be performed which mimic human body conditions.

6.5 RESULTS SECTION

Most of the discussion points for the results are already mentioned in paragraph 5.4. However, some surprising findings need to be highlighted. One of these findings is the relation between SPION size and the measured relaxivity. When the measurements of the SPION SPH25 are discarded, due to the worse goodness of fit, the biggest size SPION, SynomagD50, has the highest relaxivity ratios at 0.25 and 0.5T. This finding is somewhat surprising given that other research shows higher relaxivities ratios for smaller SPIONs [38] and advises smaller SPIONs for positive contrast.

Nevertheless, one study found that the longitudinal relaxivity increases with SPION diameter [49]. However, this research was conducted at 1.5T, while the interest of this research is for low-field. Furthermore, show the results of this research an increase in both the longitudinal and transversal relaxivity, resulting in a limited change in the relaxivity ratio.

6.6 OVERALL

The research question sought to determine if SPIONs could be used as positive contrast agents in low-field MRA. However, SPIONs are already used in other MRI applications. The SPION Ferumoxytol is already used for MRA at 1.5 and 3.0T [50]. However, this is only the case for patients diagnosed with chronic kidney disorder or renal dysfunction, for whom gadolinium-based contrast agents are not applicable. The question arises why gadolinium is still being used if another less toxic contrast agent is available? It is possible that the signal enhancement of SPIONs is not equal to that of gadolinium. In a comparative study, the SPION Ferumoxytol was compared with a gadolinium-based contrast agent in MR venography. This study found no difference in signal intensity between the two contrast agents [51]. Besides, gadolinium contrast agents quickly distribute in the extracellular fluid space after being injected into the blood pool, resulting in a very short time window to image the

vascular phase [52]. SPIONs have a prolonged intravascular circulation time of approximately 15 hours, which results in a longer window to image the vascular phase [53]. However, this long circulation time has a downside because iron particles reside for a long time in the body and could interfere with follow-up measurements. Furthermore, are the systemic side effects of SPIONs not fully understood. There is still much unknown about the long-term use of SPIONs as contrast agents, and more research must be done to substitute the embedded use of gadolinium [54].

Low-field MRI provides opportunities from which MRA research and diagnosis could benefit [4]. Firstly, upright imaging can be applied, which is beneficial because the morphology of the blood vessels in the lower extremities changes while standing up. These blood vessels can therefore be investigated using MRA. Furthermore, an 'open' MRI scanner offers opportunities for claustrophobic people who otherwise could not have an MRA scan. The development and fabrication of low-field scanners is also rising. Siemens has just put a 0.55T scanner on the market [55], and the first mobile low-field MRI scanner is also in the last stage of development [56]. Because of this development, it is essential to have sufficient contrast agents at low-field MRI.

When SPIONs are used as contrast agents, it is essential to look at the administered dosing. The dosing depends on the relaxivity of the SPION. A high relaxivity would result in a low dose of SPION. A low dose is more desirable because toxic effects are more likely to occur when using high doses. Furthermore, literature shows that the effect of the T_2 shortening increases with increasing SPION concentrations [57]; therefore, determining the optimal concentration for a specific SPION is also very important. A low concentration gives the 'best' T_1 enhancement [57]. In literature, there are multiple debates about the correct concentration of SPIONs for MRA. As mentioned before, this depends on relaxivity. However, there is a limit to the amount of iron which can be injected to stay under toxicity levels, namely 4 mg of iron per kg body weight. Therefore, when developing SPIONs for MRA, relaxivities must be sufficient to stay under this 4 mg limit.

This study shows the possibilities of using SPIONs at low-field. However, the relaxivity ratios of the measured SPIONs at low-field are not comparable to gadolinium at 1.5T. Therefore new SPIONs need to be fabricated with high r_1 and low r_2 . However, the fabrication of such SPIONs is not easy. Firstly because not all factors are known that influence relaxivity. Furthermore, if such factors are known, it is essential to fabricate particles with enhanced monodispersity [58]. However, this is not easy; further research needs to be performed to end up with the 'best' SPION for low-field MRA.

6.7 FUTURE WORK & RECOMMENDATIONS

There are still many unanswered questions about the influence of the size and coating of the SPION on the relaxivity at the different field strengths. More research on this topic needs to be undertaken before the association between the coating and relaxivity is more clearly understood. Therefore measurement could be executed with SPIONs of the same composition but different sizes or SPIONs of the same size and different compositions. This would indicate the most critical factors which influence relaxivity. Besides the coating and size influence which became clear from this research, another study shows that the pH of the blood also influences the relaxivity. A lower pH results in a higher relaxivity [59]. This factor could also be investigated in further research.

Besides the investigated field strength of 0.25, 0.5, and 1.5T, other field strengths could also be investigated to get a profile of the relaxivity of the SPIONs versus the field strength. This would give an insight into the optimal field strength of the SPIONs and also maybe give an indication of which factors result in optimal relaxivity at a specific field strength. To investigate this, it is essential to keep measuring parameters as similar as possible to keep nice comparability between the measurements.

Additional studies will be needed to develop a complete picture of contrast agent performance at low-field, not only for SPION but also for gadolinium-based contrast agents. These studies can be performed with the protocol from this research, ensuring clinically relevant measurements. However, as a result, it is advised to equalise the echo spacing of the transversal relaxation measurement to have better comparable data between the scanners of different field strengths.

Due to a lack of time to develop and optimise the protocol further, TR was chosen of 2 seconds for the measurements at 1.5 and 0.25T. However, literature has been found where imaging schemes allow for measurements with shorter TR, thereby reducing the scan time by 25% [60]. Decreasing scan time is beneficial to scanning blood samples, which must be measured as quickly as possible.

7 CONCLUSION

Returning to the question posed in the introduction, it is now possible to state that SPIONs could be used for positive contrast in low-field MRA. Chapter four has demonstrated the importance of measuring the relaxivity of contrast agents at clinically relevant conditions. Although the current study is based on only three SPIONs, the findings suggest an apparent increase in the relaxivity ratio at lower field strengths. Further research could usefully explore the influencing factors on the relaxivity to develop the best possible SPION for low-field MRA. Besides the results of the research also, the proposed methodology is useful. The methods used for determining the relaxivity may be applied to other contrast agents and SPIONs to understand additional parameters which influence the longitudinal and transversal relaxivities and, thereby, the relaxivity ratio. One of the strengths of this study is that it represents a measurements protocol for relaxivity measurements on the Esaote 0.25 T scanner, which was previously not possible. Another key finding in this research is the temperature dependency of the longitudinal relaxivity, which establishes a ground rule for further relaxivity research. To conclude, this research stated the ground rules for measuring a clinically relevant relaxivity of contrast agents and applied these rules to confirm the possibility of using SPIONs as positive contrast agents in low-field MRA.

REFERENCES

- [1] M. Hori, A. Hagiwara, M. Goto, A. Wada, and S. Aoki, "Low-Field Magnetic Resonance Imaging: Its History and Renaissance," *Invest. Radiol.*, vol. 56, no. 11, pp. 669–679, 2021.
- [2] M. P. Wattjes and F. Barkhof, "Diagnostic relevance of high field MRI in clinical neuroradiology: The advantages and challenges of driving a sports car," *Eur. Radiol.*, vol. 22, no. 11, pp. 2304–2306, 2012.
- [3] J. P. Marques, F. F. J. Simonis, and A. G. Webb, "Low-field MRI: An MR physics perspective," *J. Magn. Reson. Imaging*, vol. 49, no. 6, pp. 1528–1542, 2019.
- [4] H. Klein, S. Airport, M. Zentrum, A. Siegerlandflughafen, and C. Format, "Low-Field Magnetic Resonance Imaging," pp. 537–548, 2020.
- [5] A. E. Campbell-washburn, R. Ramasawmy, and M. C. Restivo, "Opportunities in Interventional and Diagnostic Imaging by Using High-Performance Low-Field-Strength MRI," *Radiology*, no. 3, pp. 2–11, 2019.
- [6] H. Klein, R. Buchal, U. Achenbach, and S. Domalski, "Contrast-Enhanced MRA of Carotid and Vertebral Arteries," no. 2, pp. 107–113, 2008.
- [7] C. Do *et al.*, "Gadolinium-Based Contrast Agent Use, Their Safety, and Practice Evolution," *Kidney360*, vol. 1, no. 6, pp. 561–568, 2020.
- [8] J. K. Van Zandwijk, F. F. J. Simonis, F. G. Heslinga, E. I. S. Hofmeijer, R. H. Geelkerken, and B. Haken, "Comparing the signal enhancement of a gadolinium based and an iron-oxide based contrast agent in low-field MRI," *PLoS One*, vol. 16, no. 8 August, pp. 1–12, 2021.
- [9] L. E. Minton, R. Pandit, W. R. Willoughby, and K. K. Porter, "The Future of Magnetic Resonance Imaging Contrast Agents," *Appl. Radiol.*, vol. 51, no. 1, pp. 7–11, 2022.
- [10] M. Nabavinia and J. Beltran-Huarac, "Recent Progress in Iron Oxide Nanoparticles as Therapeutic Magnetic Agents for Cancer Treatment and Tissue Engineering," *ACS Appl. Bio Mater.*, vol. 3, no. 12, pp. 8172–8187, 2020.
- [11] F. Bloch, "Nuclear induction," *Phys. Rev.*, vol. 70, no. 7–8, pp. 460–474, 1946.
- [12] D. V. Hingorani, A. S. Bernstein, and M. D. Pagel, "A review of responsive MRI contrast agents: 2005-2014," *Contrast Media Mol. Imaging*, vol. 10, no. 4, pp. 245–265, 2015.
- [13] G. J. Strijkers, W. J. M. Mulder, G. A. F. van Tilborg, and K. Nicolay, "MRI Contrast Agents: Current Status and Future Perspectives," *Anticancer. Agents Med. Chem.*, vol. 7, no. 3, pp. 291–305, 2008.
- [14] S. P. Kalva, M. A. Blake, and D. V. Sahani, "MR contrast agents," *Appl. Radiol.*, vol. 35, no. 1, pp. 18–27, 2006.
- [15] C. Burtea, S. Laurent, L. Vander Elst, and R. N. Muller, *Contrast Agents : Magnetic Resonance*, no. February. 2008.
- [16] S. Dumas *et al.*, "High Relaxivity Magnetic Resonance Imaging Contrast Agents Part 1," *Invest. Radiol.*, vol. 45, no. 10, pp. 600–612, 2010.
- [17] M. Rohrer, H. Bauer, J. Mintorovitch, M. Requardt, and H. J. Weinmann, "Comparison of magnetic properties of MRI contrast media solutions at different magnetic field strengths," *Invest. Radiol.*, vol. 40, no. 11, pp. 715–724, 2005.

- [18] V. Jacques, S. Dumas, W.-C. Sun, J. S. Troughton, M. T. Greenfield, and P. Caravan, "High-Relaxivity Magnetic Resonance Imaging Contrast Agents Part 2: Optimisation of Inner- and Second-Sphere Relaxivity," *Invest. Radiol.*, vol. 45, no. 10, pp. 613–624, 2010.
- [19] Y. Gossuin, P. Gillis, A. Hocq, Q. L. Vuong, and A. Roch, "Magnetic resonance relaxation properties of superparamagnetic particles," *Wiley Interdiscip. Rev. Nanomedicine Nanobiotechnology*, vol. 1, no. 3, pp. 299–310, 2009.
- [20] Y. Xiao and J. Du, "Superparamagnetic nanoparticles for biomedical applications," *J. Mater. Chem. B*, vol. 8, no. 3, pp. 354–367, 2020.
- [21] J. Dulińska-Litewka, A. Łazarczyk, P. Hałubiec, O. Szafranski, K. Karnas, and A. Karewicz, "Superparamagnetic iron oxide nanoparticles-current and prospective medical applications," *Materials (Basel)*, vol. 12, no. 4, 2019.
- [22] Y. Bao, J. Sherwood, Z. Sun, and J. Mater, "Magnetic Iron Oxide Nanoparticles as T1 Contrast Agents for Magnetic Resonance Imaging," *J. Mater. Chem.*, 2018.
- [23] M. Jeon, M. V Halbert, Z. R. Stephen, and M. Zhang, "Iron Oxide Nanoparticles as T 1 Contrast Agents for Magnetic Resonance Imaging : Fundamentals , Challenges , Applications , and Prospectives," vol. 1906539, pp. 1–18, 2020.
- [24] N. Nelson, J. Port, and M. Pandey, "Use of Superparamagnetic Iron Oxide Nanoparticles (SPIONs) via Multiple Imaging Modalities and Modifications to Reduce Cytotoxicity: An Educational Review," *J. Nanotheranostics*, vol. 1, no. 1, pp. 105–135, 2020.
- [25] O. Cohen and J. R. Polimeni, "Optimised inversion-time schedules for quantitative T1 measurements based on high-resolution multi-inversion EPI," *Magn. Reson. Med.*, vol. 79, no. 4, pp. 2101–2112, 2018.
- [26] K. E. Keenan *et al.*, "Multi-site, multi-platform comparison of MRI T1 measurement using the system phantom," *PLoS One*, vol. 16, no. 6 June, pp. 1–19, 2021.
- [27] D. Milford, N. Rosbach, M. Bendszus, and S. Heiland, "Mono-exponential fitting in T2-relaxometry: Relevance of offset and first echo," *PLoS One*, vol. 10, no. 12, pp. 1–13, 2015.
- [28] C. Henoumont, S. Laurent, and L. Vander Elst, "How to perform accurate and reliable measurements of longitudinal and transverse relaxation times of MRI contrast media in aqueous solutions," vol. 20, no. October, 2009.
- [29] I. Reyes-molina, A. Hernández-rodríguez, and C. Cabal-mirabal, "Methodology for determination of contrast agent relaxivity using MRI," 2022.
- [30] R. J. Ogg and P. B. Kingsley, "Optimised Precision of Inversion-Recovery T1 Measurements for Constrained Scan Time," *Magn. Reson. Med.*, vol. 51, no. 3, pp. 625–630, 2004.
- [31] B. Webb *et al.*, "Temperature dependence of viscosity, relaxation times (T1, T2) and simulated contrast for potential perfusates in post-mortem MR angiography (PMMRA)," *Int. J. Legal Med.*, vol. 131, no. 3, pp. 739–749, 2017.
- [32] K. Linghu *et al.*, "Investigations of the T1 Temperature Dependence of Protons in Water and Contrast Agents Using a High-Tc DC-SQUID-Based ULF NMR System," *IEEE Trans. Appl. Supercond.*, vol. 29, no. 4, pp. 44–47, 2019.
- [33] H. Odéen and D. L. Parker, "Magnetic resonance thermoetry and its biological applications - Physical principles and practical considerations," *Prog. Nucl. Magn. Reson. Spectrosc.*, 2019.
- [34] C. Birkl *et al.*, "Temperature dependency of T1 relaxation time in unfixed and fixed human

- brain tissue," *Biomed. Tech.*, vol. 58, no. SUPPL.1, pp. 4–6, 2013.
- [35] B. Issa, I. M. Obaidat, R. H. Hejasee, S. Qadri, and Y. Haik, "NMR relaxation in systems with magnetic nanoparticles: A temperature study," *J. Magn. Reson. Imaging*, vol. 39, no. 3, pp. 648–655, 2014.
- [36] J. L. Sondeen *et al.*, "Comparison between human and porcine thromboelastograph parameters in response to ex-vivo changes to platelets, plasma, and red blood cells," *Blood Coagul. Fibrinolysis*, vol. 24, no. 8, pp. 818–829, 2013.
- [37] A. Petrovic, A. Krauskopf, E. Hassler, R. Stollberger, and E. Scheurer, "Time related changes of T1, T2, and T2* of human blood in vitro," *Forensic Sci. Int.*, vol. 262, pp. 11–17, 2016.
- [38] P. Caravan, C. T. Farrar, L. Frullano, and R. Uppal, "Influence of molecular parameters and increasing magnetic field strength on relaxivity of gadolinium- and manganese-based T1 contrast agents," *Contrast Media Mol. Imaging*, vol. 4, no. 2, pp. 89–100, 2009.
- [39] H. T. Ta *et al.*, "Effects of magnetic field strength and particle aggregation on relaxivity of ultra-small dual contrast iron oxide nanoparticles," *Mater. Res. Express*, vol. 4, no. 11, 2017.
- [40] M. Weigel and J. Hennig, "Diffusion Sensitivity of Turbo Spin Echo Sequences," vol. 1537, pp. 1528–1537, 2012.
- [41] D. Burstein, "Stimulated echoes: Description, applications, practical hints," *Concepts Magn. Reson.*, vol. 8, no. 4, pp. 269–278, 1996.
- [42] C. L. Sammet *et al.*, "Measurement and correction of stimulated echo contamination in T2-based iron quantification," *Magn. Reson. Imaging*, vol. 31, no. 5, pp. 664–668, 2013.
- [43] R. M. Lebel and A. H. Wilman, "Transverse relaxometry with stimulated echo compensation," *Magn. Reson. Med.*, vol. 64, no. 4, pp. 1005–1014, 2010.
- [44] H. Wei *et al.*, "Exceedingly small iron oxide nanoparticles as positive MRI contrast agents," vol. 114, no. 9, pp. 2325–2330, 2017.
- [45] C. L. Meisel, P. Bainbridge, R. V. Mulkern, D. Mitsouras, and J. Y. Wong, "Assessment of Superparamagnetic Iron Oxide Nanoparticle Poly (Ethylene Glycol) Coatings on Magnetic Resonance Relaxation for Early Disease Detection," vol. 1, no. April, 2020.
- [46] N. Stikov, M. Boudreau, I. R. Levesque, C. L. Tardif, K. Barral, and G. B. Pike, "On the Accuracy of T1 Mapping : Searching for Common Ground," vol. 522, pp. 514–522, 2015.
- [47] D. P. Cistola and M. D. Robinson, "Compact NMR relaxometry of human blood and blood components," *TrAC - Trends Anal. Chem.*, vol. 83, no. Part A, pp. 53–64, 2016.
- [48] A. Yilmaz, F. Ş. Ulak, and M. S. Batun, "Proton T1 and T2 relaxivities of serum proteins," *Magn. Reson. Imaging*, vol. 22, no. 5, pp. 683–688, 2004.
- [49] T. Ahmad, H. Bae, I. Rhee, Y. Chang, J. Lee, and S. Hong, "Particle size dependence of relaxivity for silica-coated iron oxide nanoparticles," *Curr. Appl. Phys.*, vol. 12, no. 3, pp. 969–974, 2012.
- [50] J. P. Finn *et al.*, "Magnetic Resonance Angiography with Ferumoxytol," pp. 7–19, 2022.
- [51] S. Stoumpos *et al.*, "Ferumoxytol-enhanced magnetic resonance angiography for the assessment of potential kidney transplant recipients," *Eur. Radiol.*, vol. 28, no. 1, pp. 115–123, 2018.
- [52] A. Antonelli *et al.*, "New Strategies to Prolong the In Vivo Life Span of Iron-Based Contrast Agents for MRI," *PLoS One*, vol. 8, no. 10, pp. 1–17, 2013.

- [53] M. D. Hope *et al.*, "Vascular Imaging With Ferumoxytol as a Contrast Agent," vol. 205, no. September 2015, pp. 1–19, 2016.
- [54] Y. Huang, J. C. Hsu, H. Koo, and D. P. Cormode, "Repurposing ferumoxytol: Diagnostic and therapeutic applications of an FDA-approved nanoparticle," *Theranostics*, vol. 12, no. 2, pp. 796–816, 2022.
- [55] T. Rusche *et al.*, "More Space, Less Noise—New-Generation Low-Field Magnetic Resonance Imaging Systems Can Improve Patient Comfort: A Prospective 0.55T–1.5T-Scanner Comparison," *J. Clin. Med.*, vol. 11, no. 22, p. 6705, 2022.
- [56] S. C. L. Deoni *et al.*, "Development of a mobile low-field MRI scanner," *Sci. Rep.*, vol. 12, no. 1, pp. 1–9, 2022.
- [57] S. Stoumpos *et al.*, "Ferumoxytol magnetic resonance angiography: a dose-finding study in patients with chronic kidney disease," *Eur. Radiol.*, pp. 3543–3552, 2019.
- [58] Z. Shen, A. Wu, and X. Chen, "Iron Oxide Nanoparticle Based Contrast Agents for Magnetic Resonance Imaging," *Mol. Pharm.*, vol. 14, no. 5, pp. 1352–1364, 2017.
- [59] Y. Matsumoto, M. Harada, Y. Kanazawa, Y. Taniguchi, M. Ono, and Y. Bito, "Quantitative parameter mapping of contrast agent concentration and relaxivity and brain tumor extracellular pH," *Sci. Rep.*, vol. 12, no. 1, pp. 1–9, 2022.
- [60] M. Sarraçanie, "Fast Quantitative Low-Field Magnetic Resonance Imaging with OPTIMUM - Optimised Magnetic Resonance Fingerprinting Using a Stationary Steady-State Cartesian Approach and Accelerated Acquisition Schedules," *Invest. Radiol.*, vol. 57, no. 4, pp. 263–271, 2022.
- [61] H. L. Margaret Cheng, N. Stikov, N. R. Ghugre, and G. A. Wright, "Practical medical applications of quantitative MR relaxometry," *J. Magn. Reson. Imaging*, vol. 36, no. 4, pp. 805–824, 2012.

APPENDICES

APPENDIX A: SCANNER PROTOCOLS

With the points from the measurement and optimisation steps, simple protocols are made for each scanner, which are given below. Used scripts and sequences are all available on the concerned scanner.

A.1: Protocol 0.25T

This protocol is used to determine the T_1 and T_2 of a sample in different concentrations at the 0.25T Esaote scanner at the Techmed Centre at the University of Twente.

Materials:

- 0.25T Esaote MRI scanner
 - o Wrist coil
 - If no heating is needed, tubes must be fixated to a piece of Styrofoam.
 - o Knee coil
 - If heat regulation setup is used
- Concentration series of contrast agent in testing tubes
 - o Test tubes with an outer diameter of 15 mm and length of 15 cm
- Listed sequences:
 - o Scout
 - o STIR T2 A
 - o FSE

Method:

Before measuring, ensure that the sample tubes are pre-heated in a water bath of 37°C for at least 1 hour.

Measurement preparation:

1. Turn on the storing of raw data
2. Open the interface of the Esaote scanner and fill in the appropriate boxes.
3. Connect the coil to the scanner and place the sample tubes inside the coil.
4. Perform a scout and adjust the position of the samples tubes if needed

T_1 measurement

1. Open the sequence 'STIR T2 A'
2. Select the desired slice
 - a. Make sure that all tubes on the scout are circular and that no air bubbles are measured.
3. Fill in all the parameters (these are the parameters used for SynomagD50 measurements)
 - a. TR=2000 ms
 - b. TE=80 ms
 - c. FOV = 160x160 mm
 - d. Phase = 192x192
4. Fill in the first TI and start the measurement
 - a. The minimal TI is 50 ms
5. Copy the settings from the first measurement and set the second TI
6. Repeat step 4 until all desired TI are measured.

- a. The maximal TI is 2000 ms

T₂ measurement

7. Open the sequence 'FSE'
8. Copy the slice selection from the T₁ measurement.
9. Fill in all the parameters (these are the parameters used for SynomagD50 measurements)
 - a. TR=2000
 - b. FOV = 160x160 mm
 - c. Phase = 256x252
 - d. ETL=20
10. Fill in the first TE and start the measurement
 - a. The minimal TE is 20 ms. When measuring samples with relatively large T₂, a TE of 30 ms should be selected.
11. Copy the setting from the previous measurements and increase the TE by 20 ms.
 - a. Increase the TE by 30 ms if a TE of 30 ms is used first.
12. Start the FSE measurement
13. Repeat steps 11 and 12 until the maximal TE is reached
 - a. Maximum TE is the ETL multiplied by the first used TE
14. Upload the measurement to XNAT
15. Save the raw data on a USB drive or something similar
16. Turn off the storing of raw data
17. Disconnect the coil from the scanner and remove the sample tubes.

Processing the images to get the relaxation time is similar for T₁ and T₂. Only other fitting equations are used. Because this process is mainly done by script in Matlab, only the key steps will be highlighted here.

1. Load the raw data to Matlab
2. Reconstruct the STIR or FSE images
 - a. The FSE reconstruction is different from the regular reconstruction. The k-spaces of all the acquisitions are combined to get a k-space with only lines from one TE. These k-spaces can then be reconstructed to the FSE images
3. Normalise the T₁ or T₂ image series with the whole series's minimal and maximal pixel value.
4. Select the circular ROI of each sample and determine the mean signal intensity inside the ROI.
5. Plot the signal intensity versus the TI or TE to get the relaxation curve
6. Fit T₁ or T₂ to the relaxation curve.

A.2. Protocol 0.5T

This protocol is used to determine the T₁ and T₂ of a sample in different concentrations at the 0.5T tabletop scanner at the Magnetic Detection and Imaging group at the University of Twente.

Materials:

- 0.5T Tabletop scanner by Pure Devices
- Concentration series of contrast agent in testing tubes
 - o Test tubes with an outer diameter of 15 mm and length of 15 cm
- Laptop with software for directing the scanner (Matlab scripts)
 - o Open script '*Contrast_Demo_ParameterSearch*' (script 1)
 - Standard script to shim and calibrate the tabletop scanner

- Open script '*Contrast_Demo_T1*' (script 2)
 - Standard script to determine T_1
- Open script '*Contrast_Demo_T2*' (script 3)
 - Standard script to determine T_2
- Open script '*T1_estimation_KW*' (script 4)
 - Custom script to fit T_1 do data
- Open script '*T2_estimation_KW*' (script 5)
 - Custom script to fit T_2 do data

Method:

To ensure that the tabletop scanner and the water bath are at 37°C when placing the samples, they must be turned on at least one hour before starting the measurement.

After the water bath reaches 37°C, the sample tubes can be put in for at least one hour to pre-heat. If the table has reached a temperature of 37°C and the samples are pre-heated for at least one hour, measurement can be started.

T_1 measurement

1. Place the first sample in the tabletop scanner.
2. Adjust the $T1$ in script 1 to the T_{1e} of the sample and run the script.
3. Adjust the *estimated T1* in script 2 and run the script
 - a. If the measured $T1$ is not in a 50 ms range of the estimated $T1$, repeat steps 2 and 3 with measured T_1 .
4. Agitate the sample and run scripts 1 and 2 five times for multiple T_1 measurements, saving each measurement's data.
 - a. $T1 = \text{Data_first}(i).data.DateTime$
 - b. $S = \text{Data_first}(i).data.DataAmplitude$
5. Determine T_1 from the measurement data using script 4.

T_2 measurement

6. Adjust the estimated $T1$ in script 3 to the previously measured value. Set parameter *Seq.tEchoTrain* to 2 and *Seq.tEcho* to 2.3e-3.
7. Run scripts 1 and then 3
 - a. If the measurement does not show a complete MR signal decay, increase the parameter *Seq.tEcho* and repeat this step
8. Agitate the sample and run scripts 1 and 3 five times for multiple T_2 measurements, saving each measurement's data.
 - a. $TE = \text{Data_first}(i).data\{1, 1\}.DateTime$
 - b. $S = \text{Data_first}(i).data\{1, 1\}.DataAmplitude$
9. Determine T_2 from the measurement data using script 5.

A.3. Protocol 1.5T

This protocol is used to determine the T_1 and T_2 of a sample in different concentrations at the 1.5T Siemens scanner at the Techmed Centre at the University of Twente.

Materials:

- 1.5T Siemens MRI scanner
 - Head coil
- Concentration series of contrast agent in testing tubes
 - Test tubes with an outer diameter of 15 mm and length of 15 cm

- Listed sequences:
 - o Localizer
 - o t1_tse_r_tra_TI
 - o t2_se_tra_32_echoes

Method:

Before measuring, ensure that the sample tubes are pre-heated in a water bath of 37°C for at least 1 hour.

Measurement preparation:

5. Open the interface of the Siemens scanner and fill in the appropriate boxes.
6. Connect the coil to the scanner and place the sample tubes inside the coil.
7. Perform a localizer and adjust the position of the samples tubes if needed

T₁ measurement

18. Open the sequence 't1_tse_r_tra_TI'
19. Select the desired slice
 - a. Make sure that all tubes on the localizer are circular and no air bubbles are measured.
20. Fill in all the parameters (these are the parameters used for SynomagD50 measurements)
 - a. TR=2000 ms
 - b. TE=8.3 ms
 - c. FOV = 150x150 mm
 - d. Phase = 256x256
21. Fill in the first TI and start the measurement
 - a. The minimal TI is 25 ms
22. Copy the settings from the first measurement and set the second TI
23. Repeat step 4 until all desired TI are measured.

T₂ measurement

24. Open the sequence 't2_se_tra_32_echoes'
25. Copy the slice selection from the T₁ measurement.
26. Fill in all the parameters (these are the parameters used for SynomagD50 measurements)
 - a. TR=2000
 - b. FOV = 150x150mm
 - c. Phase = 256x256
 - d. TE=14.3 ms
27. Start the measurement
 - a. This sequence measures all the echoes subsequently.
28. Upload the measurement to XNAT
29. Disconnect the coil from the scanner and remove the sample tubes.

Processing the images to get the relaxation time is similar for T₁ and T₂. Only other fitting equations are used. Because this process is mainly done by script in Matlab, only the key steps will be highlighted here.

7. Load the DICOM files from XNAT to Matlab
8. Normalise the T_1 or T_2 image series with the whole series's minimal and maximal pixel value.
9. Select the circular ROI of each sample and determine the mean signal intensity inside the ROI.
10. Plot the signal intensity versus the TI or TE to get the relaxation curve
11. Fit T_1 or T_2 to the relaxation curve.

APPENDIX B: SPION PRELIMINARY TESTS

With the SPIONs selection and the dilution medium chosen, a concentration series can be made of every SPION. Preliminary relativity measurements were executed to keep the samples between the measuring limits to determine the concentration series for each SPION. Samples are made with the selected SPIONs with a concentration of 0.25, 0.5 and 1 mM in porcine blood. These samples are measured using the steps in chapter 3.

Results and discussion preliminary relativity measurements

Figure 16 shows the results of the preliminary relativity measurements of three selected SPIONs. These results are the following relaxivities found: $12.15 \text{ mM}^{-1}\text{s}^{-1}$ for EMG304, $10.56 \text{ mM}^{-1}\text{s}^{-1}$ for SPH25 and $38.95 \text{ mM}^{-1}\text{s}^{-1}$ for SynomagD50. These relaxivities give just an indication of the relativity at 0.5T. For these measurements, porcine blood was used, which was more than two days old; therefore, it could be that the 'real' relativity measurements could differ from these.

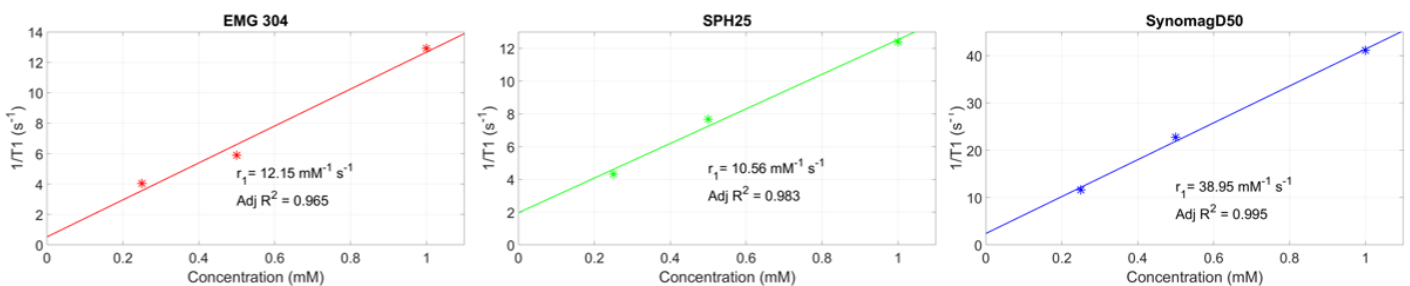


Figure 16: Resulting graph of the preliminary relativity measurements performed at 0.5T. The following relaxivities were found for each SPION: $12.15 \text{ mM}^{-1}\text{s}^{-1}$ for EMG304, $10.56 \text{ mM}^{-1}\text{s}^{-1}$ for SPH25 and $38.95 \text{ mM}^{-1}\text{s}^{-1}$ for SynomagD50

APPENDIX C: ISMRM ABSTRACT

The abstract is shown on the following pages. The figures used in the abstract are the same as those in the report and are, therefore not enlarged.

Determining the relaxivity of superparamagnetic iron oxide nanoparticles at 0.25T, 0.5T and 1.5T

Kees Wieriks¹ and Frank F.J. Simonis¹

¹Techmed Centre, University of Twente, Enschede, Netherlands

Synopsis

SPIOs show potential as contrast agents for low field MRA due to their high relaxivities and long circulation times. In this abstract the relaxivity ratio (r_1/r_2) of three SPIOs with different core size is determined at 0.25T, 0.5T and 1.5T. SPIOs were diluted in porcine blood and measured at 37°C. At 0.25T and 0.5T a higher relaxivity ratio was found for the SPIOs compared to 1.5T showing their feasibility of generating positive contrast at these field strengths.

Introduction

Low field MRI brings opportunities in the field of interventional MRI, like MRA¹. Good contrast agents (CA) are essential to image the blood vessels in MRA. Besides gadolinium superparamagnetic iron oxide nanoparticles (SPIOs) could be used as CA, because of their longer circulation time. They are already used as T_2/T_2^* contrast agents at regular field strengths, but it is hypothesized that they could be used as T_1 CA (generating positive signal) at lower magnetic fields, due to their favorable relaxivity ratio². To generate positive contrast the transverse relaxivity (r_2) mustn't be too large otherwise the signal will decay too fast in the transverse plane to create a high signal. The relaxivities values of many SPIOs in such fields are unknown and have not been tested at clinically relevant conditions, i.e. in blood and at 37°C. Therefore the scope of this work is to investigate at which field strengths SPIOs with different core diameter could generate the best contrast enhancement. To this end, the T_1 and T_2 relaxation times of the SPIOs are determined and were used to calculate both longitudinal and transversal relaxivity (r_1 and r_2) which describe their contrast-enhancing capability.

Methods

Three SPIOs were used: EMG 304 (FerroTec Corporation, USA) with a diameter of 10 nm, SPH25 (Ocean Nanotech, USA) with a diameter of 25 nm, and SynomagD50 (micro mod, Germany) with a diameter of 50 nm. Phantoms consisted of six different concentrations of SPIO dissolved in porcine blood. The T_1 and T_2 estimation measurements were performed at 0.25T (G-scan Brio, Esaote, Italy), 0.5T (Research Lab, Pure Devices, Germany), and 1.5T (Aera, Siemens Healthcare, Germany), see Figure 1. All measurements were performed at 37°C, regulated by a warming/cooling system (Variotherm 550, Hico medical systems, Germany) for the 0.25T and 1.5T measurements or regulated by the internal thermostat of the device for the measurements at 0.5T. Measurements were done on all concentrations of one SPIO simultaneously in the 0.25T and 1.5T but had to be done separately in the tabletop scanner. T_1 estimation was performed using an inversion recovery sequence. Data was fit using a three-parameter non-linear least squares curve fitting algorithm (MATLAB @2020a@, Mathworks, USA), with the following equation:

$$S = M_0(1 - 2e^{-TI/T_1}) + a$$

T_2 estimation was performed by using a multi-SE sequence for 0.5T and 1.5T scanners. For the 0.25T scanner, an FSE sequence is used, whereby lines with the same TE from different acquisitions were combined to reconstruct a single image with that effective TE. In this case the measurement data was fit to the following equation:

$$S = M_0(e^{-TE/T_2}) + a$$

Parameter settings of all experiments are given in Table 1. The relaxivities are subsequently defined as the slope of the line describing the inverse of the measured T_1 and T_2 against the SPIO concentration.

Results

The resulting r_1 and r_2 are shown in the graphs of Figures 2 and 3. The r_1 's at a field strength of 1.5T are at least 2 times lower compared to a field strength of 0.25 T and even 5 times lower compared to 0.5T. The r_2 's at a field strength of 1.5T are lower compared to the other field strengths. However, this difference is less prominent. In Table 2 an overview is given of all ratios of relaxivity. For every SPIO the r_1/r_2 ratio is very low at 1.5 T, which will result in negative contrast. At lower fields, this ratio is higher, with a maximum of 0.27 for SPH25 at 0.25T. Measurements on a gadolinium-based contrast agent (Dotarem) were added from literature^{2,3} for comparison. Although the relaxivity ratio of the gadolinium-based CA is more than 10 times higher at 1.5T, it is lower at 0.25T when compared with the SPIOs SPH25 and SynomagD50.

Discussion

The relaxivity ratio was expected to be highest for the EMG304 because of its smaller diameter, which results in lower magnetization⁴. However, the other SPIOs have higher relaxivity ratios at 0.25 and 0.5T. This could be due to some measuring error during the EMG304 measurements. Nevertheless, the r_1 and r_2 fit of EMG304 show an adjusted R-square higher than 0.88, from which it can be assumed that the measurements are supposed to be performed properly. One explanation could be that the optimal field strength for EMG304 is higher than expected, but this should be further investigated. In Figure 3 it is seen that the adjusted R-square of the SPH25 measurements on 0.25T is lower than the other SPIOs. This could be explained by the fact that fewer data points were used for the T_2 measurements and therefore the T_2 estimation is less accurate. However, when you combine all the results, the SPIOs show a high r_1 and r_2 (which results in lower dose administrating and a favorable relaxivity ratio compared to gd at low field strengths).

Conclusion

From this research, it can be suggested that SPIOs could be used for positive contrast due to their relaxivity ratio at low magnetic field strengths. This ratio is SPIO dependent. In this research, SPH25 has the highest relaxivity ratio at 0.25T and SynomagD50 at 0.5T. Because of the positive contrast and long circulation time SPIOs could be a viable alternative to gadolinium-based CA in low field MRA.

Acknowledgements

The authors would like to acknowledge Andrea Girardi, Luca Balbi, and Fabrizio Ferrando for their support with the Esaote raw data processing. The authors also want to thank W.J. Leppink for his involvement in the process of designing the heat regulation system.

References

1. Campbell-washburn AE, Ramasawmy R, Restivo MC. Opportunities in Interventional and Diagnostic Imaging by. Radiology. 2019;(3):2-11.
2. Van Zandwijk JK, Simonis FFJ, Heslinga FG, Hofmeijer EIS, Geelkerken RH, Haken B. Comparing the signal enhancement of a gadolinium based and an iron-oxide based contrast agent in low-field MRI. PLoS One [Internet]. 2021;16(8 August):1-12.
3. Rohrer M, Bauer H, Mintorovitch J, Requardt M, Weinmann HJ. Comparison of magnetic properties of MRI contrast media solutions at different magnetic field strengths. Invest Radiol. 2005;40(11):715-24.
4. Waddington DEJ, Boele T, Maschmeyer R, Kuncic Z, Rosen MS. High-sensitivity in vivo contrast for ultra-low field magnetic resonance imaging using superparamagnetic iron oxide nanoparticles. Sci Adv. 2020;6(29):1-10.

Figures



Figure 1: Overview of the used scanners. A: 0.25 T MRI scanner (G-scan Brio, Esaote, Italy). B: 0.5 T tabletop scanner (Magspec, Pure devices, Germany). C: 1.5 T MRI scanner (MAGNETOM Area, Siemens, Germany). A1: A cropped image of SPH25 phantoms at 0.25T with positive contrast. (TR=2000 ms, TE 80 ms, 0.58x0.58x5.0mm).

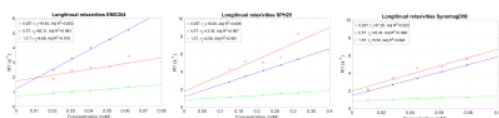


Figure 2: Longitudinal (r_1) relaxivities of the measured SPIONs at 0.25T, 0.5T, and 1.5T. Adjusted R-square is given to indicate the goodness of the fit of the relaxivity.

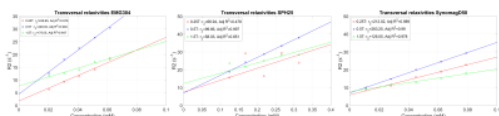


Figure 3: Transversal (r_2) relaxivities of the measured SPIONs at 0.25T, 0.5T, and 1.5T. Adjusted R-square is given to indicate the goodness of the fit of the relaxivity.

Field strength	Sequence	TR (ms)	TE (ms)	TI (ms)	Voxel size (mm)
T ₁	IR	2000	80	50, 100, 150, 200, 250, 300, 350, 500, 750, 1000, 1500 & 1850	0.70x0.70x5.0
	IR	5 x estimated T ₁	—	3 to TR, increased logarithmically	15.0x15.0x15.0
	IR	2000	8.3	25, 50, 100, 150, 200, 250, 300, 350, 500, 750, 1000, 1250, 1500 & 1950	0.59x0.59x5.0
T ₂	Sequence	TR (ms)	ETL	TE (ms)	Voxel size (mm)
	FSE	2000	20	20 up to 400*	0.63x0.63x5.0
	Multi SE	5 x estimated T ₂	500	4 up to 2000	15.0x15.0x15.0
1.5T	Multi SE	2000	32	14.3 up to 457.6*	0.59x0.59x5.0

Table 1: Parameter settings of the three scanners during the different SPION measurements. *The TE was changed after the measurements of the SPION SPH25 to increase the number of data points. For the SPH25 measurements, the TE ranged from 30 to 600 ms at 0.25T. The echo train at 1.5T started at 15 ms.

Field strength	r ₁ /r ₂	EMG304	SPH25	SynomagD50	Dotarem
0.25T		0.079	0.270	0.222	0.166 ²
0.5T		0.152	0.136	0.153	
1.5T		0.055	0.044	0.044	0.627 ³

Table 2: Calculated relaxivity ratio (r_1/r_2) for each SPION. Values for Dotarem were extracted from literature ^{2,3}. The relaxivity ratio of all SPIONs increases from high to low field, which makes them beneficial for positive contrast.